ClusComp: A Simple Paradigm for Model Compression and Efficient Finetuning

Anonymous ACL submission

Abstract

As large language models (LLMs) scale, model compression is crucial for edge deployment and accessibility. Weight-only quantization reduces model size but suffers from performance degradation at lower bit widths. Moreover, standard finetuning is incompatible with quantized models, and alternative methods often fall short of full finetuning. In this paper, we propose *ClusComp*, a simple yet effective compression paradigm that clusters weight matrices into codebooks and finetunes them block-by-block. ClusComp (1) achieves superior performance in 2-4 bit quantization, (2) pushes compression to 1-bit while outperforming ultra-low-bit methods with minimal finetuning, and (3) enables efficient finetuning, even surpassing existing quantization-based approaches and rivaling full FP16 finetuning. Notably, ClusComp supports compression and finetuning of 70B LLMs on a single A6000-48GB GPU.

1 Introduction

Large language models (LLMs) have garnered significant acclaim and success across various domains and applications (Dubey et al., 2024; Brown et al., 2020; Raffel et al., 2020a). With ongoing advancements, the scope and complexity of released LLMs have witnessed exponential growth, with some LLMs encompassing >50B parameters (DeepSeek-AI et al., 2024; Zhang et al., 2022; Scao et al., 2022). This remarkable upscaling introduces considerable challenges, particularly when deploying these models or granting their accessibility to users with constrained resources. To address these challenges, weight-only post-training quantization (PTQ) has emerged as an effective approach.

PTQ methods can generally be classified into three categories: statistic-based, gradient-based, and codebook-based approaches. Statistic-based methods (Dettmers et al., 2024; Lin et al., 2024; Frantar et al., 2022) determine the quantization grid based on the weight value distribution, whereas gradient-based methods (Shao et al., 2024; Ma et al., 2024) optimize the quantization grid with some calibration samples. Codebook-based methods (Egiazarian et al., 2024; van Baalen et al., 2024; Kim et al., 2024; Park et al., 2024) cluster similar weight elements to the shared quantized centroids, employing non-uniform quantization and pushing the limits to extremely low bit levels. However, these methods continue to struggle with low-bit quantization and the presence of outliers in weights, leading to significant performance degradation.

Another challenge PTQs encounter is their limited support for finetuning, which is crucial for adapting LLMs to various downstream tasks. Finetuning LLMs is computationally expensive due to their large scale and the need to cache activations and store optimizer states. PTQ, which compresses LLMs, appears to be a promising approach for finetuning as it reduces the memory requirements for loading LLMs. However, most quantization techniques use a round-to-nearest operation, which does not support gradient backpropagation. Typically, parameter-efficient methods (Dettmers et al., 2023; Li et al., 2024c; Liao and Monz, 2024b) are employed to train the added parameters while keeping the quantized LLMs frozen, bypassing this limitation. However, this fine-tuning approach presents two major drawbacks: (1) freezing quantized LLMs prevents further reduction of quantization errors during finetuning; (2) The low-rank nature of most parameter-efficient methods restricts their expressiveness (Biderman et al., 2024; Liao and Monz, 2024a).

In this paper, we propose a simple while effective paradigm that mainly applies **Clus**tering to **Comp**ress LLMs, referred to as *ClusComp*. Additionally, ClusComp can function as a parameter and memory-efficient finetuning method. Our preliminary experiments reveal that LLMs are increasingly difficult to quantize, mainly due to the growing fre-

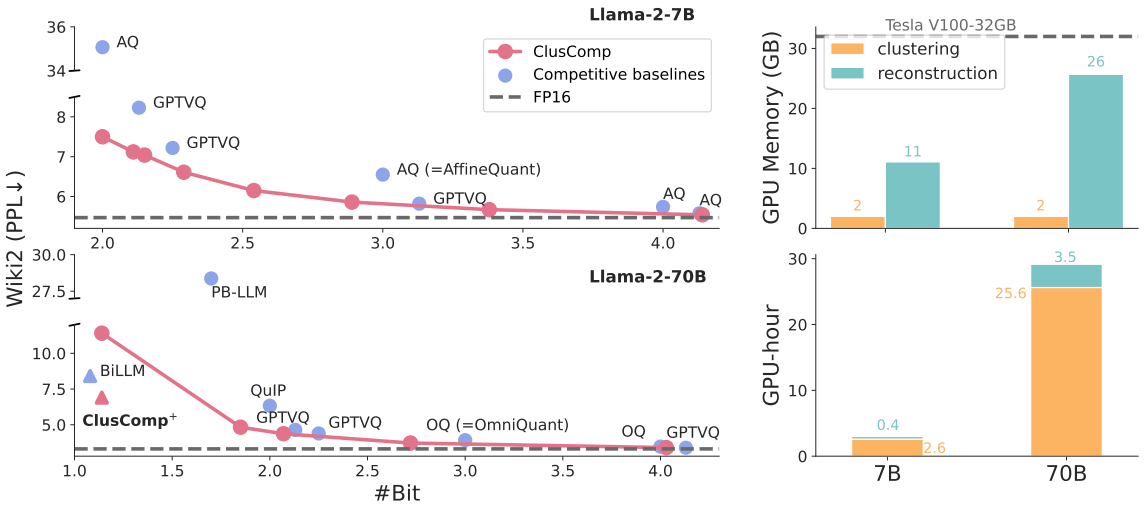

Figure 1: **Left:** Compression quality of ClusComp. Only the most competitive baselines are shown here. Please refer to Table A.1 and A.2 for a full comparison. Methods in triangle use more calibration samples than the ones in circle. **Right:** Compression efficiency of ClusComp that consists of sequential clustering and reconstruction steps. E.g., compressing a 70B LLM takes 25.6h + 2GB for clustering, and 3.5h + 26GB for reconstruction on 1 GPU.

quency of outliers in their weight matrices (§3). Based on this observation, we propose using clustering instead of quantization to compress LLMs, retaining all values in FP16 format to circumvent issues arising from outlier quantization (§3.1). To further reduce compression errors, we minimize block-wise output discrepancies between the compressed and uncompressed blocks, using a limited set of calibration samples (§3.3). In addition, by incorporating an inexpensive end-to-end recovery finetuning step, we can even push the compression rate to the 1-bit level. Since all parameters remain in FP16 after compression, ClusComp fully supports standard neural training, thus allowing the seamless finetuning of compressed LLMs on various downstream tasks (§3.4).

We begin by evaluating the effectiveness of ClusComp in the context of model compression across 2 language modeling tasks and 6 zero-shot reasoning tasks. ClusComp consistently surpasses various baselines at 2-4 levels, even achieving a perplexity of <13 at the 2-bit level on WikiText2 (Merity et al., 2017) for all LLMs (§4.1). Following recovery finetuning, ClusComp's performance at 2-bit and 1-bit levels approaches that of the FP16 model, with an accuracy of 57.8 vs 68.6 for the 2-bit Llama-3-8B and 51.4 vs 75.4 for the 1-bit Llama-3-70B (§4.2). Additionally, ClusComp demonstrates its utility as a parameter-efficient ($< 1\%$) and memory-efficient (42GB for Llama-3-70B) finetuning method, outperforming quantization-based and memory-efficient finetuning approaches, while matching the performance of full finetuning (§4.3).

2 Related Works

Quantization refers to the process of converting floating-point values into discrete levels, thereby reducing the bit-width required and minimizing memory consumption during model loading. Taking the symmetric uniform quantization as an example, a weight matrix $\boldsymbol{W}$ is quantized as follows:

$$\boldsymbol{W}_q = \text{clamp}(\lfloor \frac{\boldsymbol{W}}{s} \rceil, -2^{b-1}, 2^{b-1} - 1)$$

where the scale factor $s = \frac{\max(|\boldsymbol{W}_{\min}|, |\boldsymbol{W}_{\max}|)}{2^b - 1}$, b denotes the bit-width, and $\lfloor \rceil$ represents the round-to-nearest (RTN) operation. Since the quantization grid is uniform, its effectiveness is contingent on the distribution of the weight values. In cases where the weight matrix contains a significant number of outliers or is quantized to lower bit-widths, the resulting quantization error may be substantial.

Post-training quantization (PTQ) methods, such as GPTQ (Frantar et al., 2022), AWQ (Lin et al., 2024), and OmniQuant (Shao et al., 2024), apply quantization to a model after training with minimal computational resources. However, these approaches, which rely on uniform quantization, are significantly impacted by the presence of outliers in the weight matrices. Recent methods (Dettmers et al., 2024; Yuan et al., 2024; Huang et al., 2024a) address this challenge by retain-

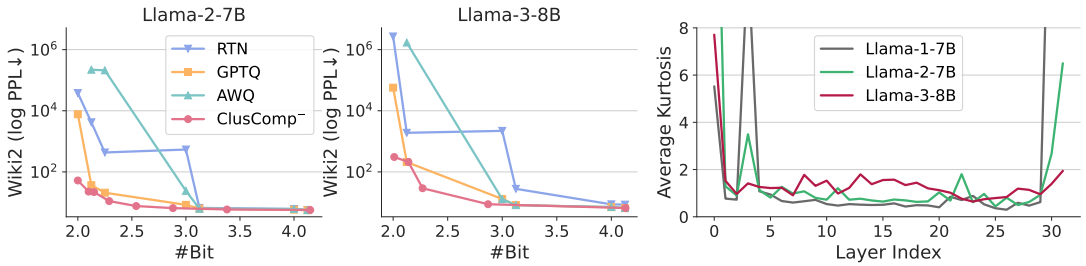

Figure 2: The Llama series becomes progressively harder to quantize. **Left** & **Middle:** From Llama-2 to Llama-3, all methods struggle more with lower-bit quantization, though ClusComp$^-$ is the least affected. **Right:** From Llama-1 to Llama-3, the average weight kurtosis across most layers increases.

ing salient weights in FP16 format, thereby maintaining strong performance at lower bit widths. Nonetheless, these mixed-precision quantization techniques require specially optimized CUDA kernels to either enhance or preserve inference speed. Closely related to our proposed method, ClusComp, are works such as GPTVQ (van Baalen et al., 2024), QuIP# (Tseng et al., 2024) and SqueezeLLM (Kim et al., 2024) which implement quantized codebooks for non-uniform quantization, achieving state-of-the-art performance for ultra-low-bit quantization. ClusComp, however, differs in two significant ways: (1) The codebook in ClusComp is stored in FP16, offering additional advantages for subsequent recovery training and finetuning; (2) While other methods face limitations similar to those in VAE-like approaches (Kingma and Welling, 2014), where large and high-dimensional codebooks are infeasible due to mode collapse, ClusComp circumvents this issue. Our fixed-code design allows us to utilize a codebook size of 2^{16} in 4-16D without encountering such difficulty.

Finetuning is crucial for adapting LLMs to various domains and applications. Quantization, which reduces model size, is theoretically more conducive to finetuning. However, directly finetuning a quantized model is not a standard approach, as RTN does not support gradient backpropagation. Finetuning using a straight-through estimator (STE) (Bengio et al., 2013) is relatively underexplored and may lead to catastrophic forgetting (Malinovskii et al., 2024). Previous works (Xu et al., 2024a; Liao and Monz, 2024b; Dettmers et al., 2023) propose freezing the quantized model while updating newly added LoRAs (Hu et al., 2022). However, these approaches suffer from two key limitations: (1) Freezing the quantized model prevents the mitigation of quantization errors during finetuning. Moreover, not all quantization methods are suitable for finetuning. Popular techniques like GPTQ and QLoRA, while widely used, exhibit significant quantization errors below 4-bit. (2) The expressiveness of LoRA is constrained by its bottleneck design (Biderman et al., 2024; Liao and Monz, 2024a). In contrast, ClusComp, where all parameters are maintained in high precision, inherently supports seamless finetuning. Additionally, updating the codebook in ClusComp results in modifying all parameters in the weight matrices, even offering superior performance compared to full finetuning while maintaining a similar number of trainable parameters as LoRA.

3 ClusComp

Pilot study. Before introducing ClusComp, we present a key observation from our experiments on different Llama series. As in Figure 2 (Left & Middle), when reducing the bit-width, the performance of various quantization methods (RTN, GPTQ, and AWQ) follows a similar trend: Llama-3 (Dubey et al., 2024) proves more challenging to quantize than Llama-2 (Touvron et al., 2023b).

We hypothesize that the increasing quantization difficulty stems from a higher frequency of outliers in Llama-3's linear layers. Since these methods rely on uniform quantization, they are particularly sensitive to outliers in weight matrices. To test this, we analyzed the kurtosis of weight matrices—a well-established metric for detecting outliers (Bondarenko et al., 2023). As shown in Figure 2 (Right), we observe: (1) Higher kurtosis at the beginning and end of all models; (2) A consistent increase in kurtosis from Llama-1 to Llama-3 across most layers, indicating more frequent outliers. This trend likely explains the growing quantization challenge and suggests that future Llama models may be even harder to quantize.[1]

[1]Further discussion and proof are in §A.1.

Since quantization performance is affected by outliers, could an alternative compression approach involve storing all weight values in FP16 rather than applying quantization?

The first idea that comes to mind is clustering, where similar weight values are represented by a single shared value. This approach enables model compression while maintaining all weight values in FP16. In the following, we introduce three ClusComp variants that leverage clustering for LLM compression: *ClusComp*$^-$, which applies clustering alone; *ClusComp*, which enhances ClusComp$^-$ with block-wise error minimization; and *ClusComp*$^+$, which further refines the compressed model through next-token prediction.

3.1 ClusComp$^-$: Clustering

Considering a weight matrix $\boldsymbol{W} \in \mathbb{R}^{d_{\text{in}} \times d_{\text{out}}}$, direct clustering along either dimension of $\boldsymbol{W}$ is suboptimal as it leads to a significant reconstruction error, particularly due to the large values of d_{in} and d_{out} in LLMs. To mitigate this issue, we reshape $\boldsymbol{W}$ into a set of lower-dimensional vectors, denoted as $\boldsymbol{W}' = \{\boldsymbol{w}_1, \boldsymbol{w}_2, \ldots, \boldsymbol{w}_k\}$, where each $\boldsymbol{w}_i \in \mathbb{R}^g$ and $k = \frac{d_{\text{in}} \cdot d_{\text{out}}}{g}$.[2] The goal is to partition $\boldsymbol{W}'$ into n clusters $\{C_1, C_2, \ldots, C_n\}$ by solving the following optimization problem:

$$\text{argmin}_{\{C_1, C_2, \ldots, C_n\}} \sum_{j=1}^{n} \sum_{\boldsymbol{w}_i \in C_j} ||\boldsymbol{w}_i - \boldsymbol{c}_j||^2$$

where $\boldsymbol{c}_j \in \mathbb{R}^g$ denotes the centroid of cluster C_j. This clustering problem is well-established in the machine learning literature and can be iteratively addressed using K-means (Lloyd, 1982) with the Expectation-Maximization (EM) algorithm:

- **E-step**: Each vector $\boldsymbol{w}_i$ is assigned to the cluster whose centroid $\boldsymbol{c}_j$ minimizes the Euclidean distance, i.e., $C_j^{(t)} = \{\boldsymbol{w}_i : ||\boldsymbol{w}_i - \boldsymbol{c}_j^{(t)}||^2 \leq ||\boldsymbol{w}_i - \boldsymbol{c}_l^{(t)}||^2 \quad \forall l\}$.
- **M-step**: The centroid of each cluster is updated as the mean of the vectors assigned to that cluster, i.e., $\boldsymbol{c}_j^{(t+1)} = (\sum_{\boldsymbol{w}_i \in C_j^{(t)}} \boldsymbol{w}_i)/|C_j^{(t)}|$.

Upon completion, two key elements are obtained for each weight matrix: (1) a codebook $\boldsymbol{C} = \{\boldsymbol{c}_1, \boldsymbol{c}_2, \ldots, \boldsymbol{c}_n\} \in \mathbb{R}^{g \times n}$ that contains all centroids, and (2) a set of codes $\boldsymbol{q} = \{q_1, q_2, \ldots, q_k\} \in \{1, 2, \ldots, n\}^k$ that records the assignment of each vector $\boldsymbol{w}_i$ to the closest centroid, where $q_i = q(\boldsymbol{w}_i) = j$ if $\boldsymbol{c}_j = \text{argmin}_{\boldsymbol{c}_l \in \boldsymbol{C}} ||\boldsymbol{w}_i - \boldsymbol{c}_l||^2$. Using the codes $\boldsymbol{q}$ and the codebook $\boldsymbol{C}$, the weight matrix $\boldsymbol{W}'$ can be reconstructed as $\hat{\boldsymbol{W}}' = \{\boldsymbol{c}_{q_1}, \boldsymbol{c}_{q_2}, \ldots, \boldsymbol{c}_{q_k}\}$. In PyTorch (Paszke et al., 2017), the linear layer is adapted as in Listing 1.

Remark: ClusComp, when applied solely with clustering, is referred to as ClusComp$^-$. In this configuration, only the weight matrices (no calibration samples) are utilized, leading to substantial memory efficiency, with a mere 2GB memory consumption for both 7B and 70B LLM on 1 GPU, as shown in Figure 1. Moreover, this process can be considerably accelerated with more GPUs, as the clustering of different matrices is independent.

Setting	#Params. for Codes	#Params. for Codebook	$\bar{b}$
g4n65500	4.19M	0.26M (1.55%)	4.25
g6n65500	2.80M	0.39M (2.32%)	3.04
g9n65500	1.86M	0.59M (3.52%)	2.34

Table 1: Bits for $\boldsymbol{W}$ with $d_{\text{in}}, d_{\text{out}} = 4096$ (16.78M).

3.2 Estimate model size

After clustering, it is sufficient to store the codes $\boldsymbol{q} \in \{1, 2, \ldots, n\}^k$ and codebook $\boldsymbol{C} \in \mathbb{R}^{g \times n}$. Unlike prior works (van Baalen et al., 2024; Egiazarian et al., 2024; Tseng et al., 2024), we don't quantize the codebook; instead, we store it in the FP16 format. The bit-width required for the codes depends on the range of n. To maintain efficiency, we set $n < 2^{16}$ and use unsigned 16-bit integers to represent the codes. Thus, the average bits-per-parameter is calculated as:

$$\bar{b} = \frac{\text{size in bits}}{\text{number of parameters}} = \frac{16 \cdot k + 16 \cdot g \cdot n}{d_{\text{in}} \cdot d_{\text{out}}} = \frac{16}{g} + \frac{16 \cdot g \cdot n}{d_{\text{in}} \cdot d_{\text{out}}} \quad (1)$$

In the right-most of Equation (1), the first term corresponds to the bit-width allocated to the codes, and the second term corresponds to the bit-width of the codebook. E.g., for a linear layer $\boldsymbol{W}$ with $d_{\text{in}} = d_{\text{out}} = 4096$, clustering with $g = 4$ and $n = 2^{16} - 1$ results in $\bar{b} \approx 4 + 0.25 = 4.25$. This demonstrates that the majority of the bit-width is allocated to the codes, which is a primary reason for constraining $n < 2^{16}$, so we can use 16 instead

[2] In cases where the dimensions are not divisible, zero-padding is applied to $\boldsymbol{W}$. In PyTorch, the matrix is reshaped as $\boldsymbol{W}' = \boldsymbol{W}$.transpose(1, 0).view(-1, g), where transposing $\boldsymbol{W}$ offers slightly better performance.

of 32-bit integers to represent the code. Further reducing n to a smaller range leads to fewer centroids, which in turn increases reconstruction error. More settings can be found in Table 1 and A.1.

Remark: While we express the model size in terms of bits-per-parameter, it is important to note that no quantization is applied in ClusComp. Instead, we reduce the number of parameters in $\boldsymbol{W}$ from $d_{\text{in}} \cdot d_{\text{out}}$ to $k + g \cdot n$. Utilizing bits-per-parameter allows for a direct comparison between ClusComp and quantization-based methods. Surprisingly, ClusComp$^-$, which only incorporates the clustering step without employing any calibration data, already surpasses RTN, GPTQ and AWQ, as illustrated in Figure 2 (Left & Middle).

3.3 ClusComp: Block error minimization

Block-wise error minimization (block-wise reconstruction or knowledge distillation) has emerged as a standard, efficient and effective approach to reducing quantization error (Egiazarian et al., 2024; Tseng et al., 2024; van Baalen et al., 2024; Shao et al., 2024; Liao and Monz, 2024b). To further mitigate the compression error caused by clustering, we incorporate block-wise error minimization into ClusComp$^-$ using a limited set of calibration samples, expressed as:

$$\text{argmin}_{\boldsymbol{C}s} ||\mathcal{F}(\boldsymbol{W}s, \boldsymbol{X}) - \mathcal{F}(\boldsymbol{C}s, \boldsymbol{q}s, \boldsymbol{X}')|| \quad (2)$$

Here, $\mathcal{F}$ denotes a Transformer block (Vaswani et al., 2017), $\boldsymbol{W}$s represent the weight matrices in the uncompressed block, and $\boldsymbol{C}$s and $\boldsymbol{q}$s denote the codebooks and codes in the compressed block. $\boldsymbol{X}$ refers to the input of the uncompressed block, which is also the output from the previous uncompressed block, while $\boldsymbol{X}'$ is the input to the compressed block, originating from the output of the preceding compressed block. For the first block, we have $\boldsymbol{X} = \boldsymbol{X}'$. Block-wise error minimization is memory-efficient as it only requires loading two blocks into the GPU simultaneously.

Remark: In Equation (2), we only train the codebook $\boldsymbol{C}$s while keeping the codes $\boldsymbol{q}$s fixed as indices. This design offers two key advantages: (1) It enhances data efficiency. As illustrated in Table 1, the majority of parameters are represented by the codes. Training both the codebooks and codes with a limited number of calibration samples (128) leads to overfitting; (2) More importantly, training the codes with a large number of centroids (2^{16}) can result in mode collapse (Sun et al., 2024b; Kingma and Welling, 2014). Since the codes already exhibit a uniform distribution after clustering (see Figure A.2), keeping the codes fixed indicates that all centroids in the codebook can be trained uniformly. Such a code-fixed design is also applied to the following recovery and finetuning step. Combining both clustering and block-wise error minimization steps, we term this method ClusComp.

3.4 ClusComp$^+$: Recovery and finetuning

We present the adapted linear layer for ClusComp in Listing 1, which can be seamlessly integrated as a replacement for the original linear layer in LLMs. As the codebook is represented in FP16, this new layer inherently supports training without requiring additional tricks, like STE.

Recovery training. The compressed LLMs can be further trained by predicting the next token to recover information lost due to compression. This is achieved by finetuning the codebook parameters. This form of training is memory-efficient in two distinct ways: (1) Since the LLM is already compressed, loading it onto the GPU consumes less memory compared to the FP16 version; (2) As illustrated in Table 1, the parameters in the codebook account for $< 5\%$ of the total parameters in the FP16 version, making the training both parameter-efficient and memory-efficient. We refer to ClusComp with recovery training as ClusComp$^+$.

Finetuning. Like recovery training, finetuning the compressed LLM on downstream tasks can also be performed efficiently. Unlike QLoRA (Dettmers et al., 2023), which freezes the quantized LLM and trains only the LoRA (Hu et al., 2022) modules, finetuning the codebook alone eliminates the need for this additional constraint. This approach offers two key advantages over QLoRA: (1) Freezing the quantized LLM prevents mitigation of quantization errors, whereas finetuning the codebook can further address compression errors for downstream tasks; (2) The low-rank bottleneck of LoRA limits its expressiveness (Biderman et al., 2024). In contrast, finetuning the codebook is analogous to adapting the entire high-rank weight matrix, providing greater flexibility and expressiveness.

4 Experiments

4.1 Compression results

LLMs and evaluation. We evaluate ClusComp on widely adopted LLM families: Llama-1-7B, Llama-2-7B/13B/70B and Llama-3-8B/70B (Tou-

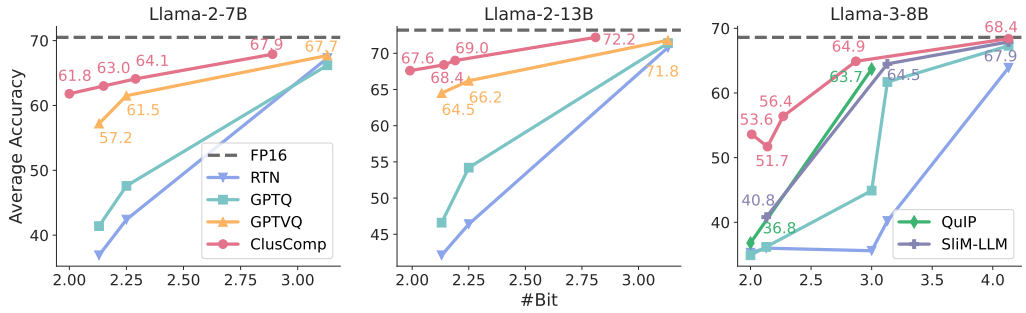

Figure 3: Average zero-shot accuracy over 5 or 6 commonsense reasoning tasks, only including competitive baselines. Please refer to Table A.3 and A.4 for detailed numbers and the full comparison.

Method	#Bit	AI2D ↑	ChartQA ↑	DocVQA ↑	MMBench ↑	Avg ↑	MME (cog / per) ↑
LLaVA-Next-8B	16.00	71.7	69.2	78.2	72.2	72.8	1965.1 (376.8 / 1588.3)
GPTQ	4.13	**70.7**	67.4	77.4	71.0	71.6	1895.0 (331.6 / 1563.4)
AWQ	4.13	70.6	68.0	77.2	**71.1**	71.7	1888.4 (325.7 / 1562.7)
ClusComp	4.13	70.0	**68.7**	**77.6**	**71.1**	**71.8**	**1915.7** (322.1 / 1593.6)
GPTQ	3.13	66.2	65.1	**75.6**	67.4	68.6	1831.8 (290.1 / 1541.7)
AWQ	3.13	67.7	65.4	74.4	**68.0**	68.9	1840.3 (298.6 / 1541.7)
ClusComp	**2.87**	**68.7**	**65.8**	74.8	67.7	**69.3**	**1872.6** (331.1 / 1541.5)
GPTQ	2.13	0.0	0.0	0.0	0.0	0.0	0.0 (0.0 / 0.0)
AWQ	2.13	0.0	0.0	0.0	0.0	0.0	0.0 (0.0 / 0.0)
ClusComp	2.14	**53.9**	**53.1**	**56.7**	**50.1**	**53.5**	**1673.0** (294.6 / 1378.4)

Table 2: Zero-shot multimodal evaluation, with baseline results from Huang et al. (2024c).

vron et al., 2023a,b; Dubey et al., 2024). We measure the performance of compressed LLMs on zero-shot and language modeling tasks. For zero-shot evaluation, we apply 6 tasks from lm-eval v0.4.4 (Gao et al., 2024), i.e. PIQA (Bisk et al., 2020), ARC-e/c (Clark et al., 2018), BoolQ (Clark et al., 2019), HellaSwag (Zellers et al., 2019) and WinoGrande (Sakaguchi et al., 2020). For language modeling, we report the perplexity on the whole test set of WikiText2 (Merity et al., 2017) and on 256 samples from the validation set of C4 (Raffel et al., 2020b) with a sequence length of 2048 as our baselines. We also apply ClusComp to LLaVA-Next-8B (Li et al., 2024b), and evaluate it on 5 multimodal tasks from lmms-eval v0.2.3 (Li et al., 2024a) to show its broad applicability, i.e. AI2D (Kembhavi et al., 2016), ChartQA (Masry et al., 2022), DocVQA (Mathew et al., 2021), MMBench (Liu et al., 2023) and MME (Yin et al., 2023).

Baselines. Here we primarily compare ClusComp with three categories of baselines: (1) statistic-based methods without neural training, including vanilla RTN, GPTQ (Frantar et al., 2022), AWQ (Lin et al., 2024), and PB-LLM (Yuan et al., 2024);[3] (2) gradient-based methods with neural training (such as block-wise distillation), including OmniQuant (Shao et al., 2024), AffineQuant (Ma et al., 2024), and SliM-LLM$^+$ (Huang et al., 2024b); and (3) quantized codebook-based methods, including QuIP (Chee et al., 2023) and GPTVQ (van Baalen et al., 2024). All baseline results are directly borrowed from the original works or their follow-up works.

Settings. We begin by applying K-means clustering to the weight matrices in all linear layers, referring to this method as ClusComp$^-$. Next, we use 128 samples from the WikiText2 training set to minimize block-wise error through codebook training only, which we denote as ClusComp. It is important to note that the majority of the aforementioned baselines utilize resources comparable (GPU memory and the number of calibration samples) to those used in ClusComp. Please refer to §B for all experimental details in this section.

Results. The main language modeling results are shown in Figure 1. At the 4-bit level, all methods are comparable. At bit-widths < 4, ClusComp consistently outperforms all baselines, with a larger gap for a lower bit-width. Notably, even at the 2-bit level, ClusComp's perplexity remains within a functional range, < 13 on WikiText2. Figure 3 presents the zero-shot evaluation results, where ClusComp again consistently surpasses all baselines across different bit-widths. Furthermore, ClusComp exhibits significantly less sensitivity to

[3] ClusComp$^-$ is also a statistic-based method.

Method	#Bit	Avg. Acc↑	Method	#Bit	Avg. Acc↑
Llama-2-7B	16.00	64.8	**Llama-2-13B**	16.00	67.8
QuiP#	2.02	57.5	QuiP#	2.01	61.5
AQLM	2.02	56.5	AQLM	1.97	60.6
ClusComp	2.00	56.6	ClusComp	1.99	62.0
ClusComp$^+$	2.00	**57.8**	**ClusComp$^+$**	1.99	**63.1**
Llama-3-8B	16.00	68.6	**Llama-3-70B**	16.00	75.4
QuiP	2.00	36.8	QuIP	2.00	48.7
PB-LLM	2.00	38.8	PB-LLM	1.70	44.1
DB-LLM	2.00	51.8	BiLLM	1.10	44.2
ClusComp	2.01	53.6	ClusComp	1.14	39.7
ClusComp$^+$	2.01	**57.8**	**ClusComp$^+$**	1.14	**51.4**

Table 3: Zero-shot accuracy on ultra-low-bit LLMs. Please refer to Table A.5 for accuracy on various tasks.

Method	Bit	#Trained	MMLU 5-shot ↑	AGIEval 3-shot ↑
Llama-2-7B	16.00	-	45.9	25.7
Full FT	16.00	100%	45.7	27.0
LoRA ($r = 128$)	16.00	4.9%	45.5	24.7
GaLore	16.00	100.0%	45.5	24.4
LISA	16.00	100.0%	46.2	26.1
ClusComp	4.15	0.9%	**47.0**	**26.5**
ClusComp	2.88	1.4%	45.1	25.6
ClusComp	2.00	1.4%	30.7	21.8

Table 4: ClusComp performance against efficient finetuning, with baseline results from Pan et al. (2024).

bit-width variations, as indicated by the flatter slope of its accuracy curve.

We also compress the Llama-3-8B backbone in LLaVA-Next-8B, and report the zero-short performance in Table 2. On average, ClusComp continues to outperform both GPTQ and AWQ, while using a comparable or even lower number of bits. A particularly noteworthy observation occurs at the 2-bit level, where none of the baselines produce correct outputs, whereas ClusComp retains strong performance. In comparison to the 2-bit results for Llama-3-8B in Figure 3 (Right), this suggests that quantizing multimodal models presents unique challenges, warranting further study.

4.2 Push the limit of model compression

We further enhance the performance of 2-bit LLMs and extend the compression boundary to the 1-bit level through efficient recovery training. This is achieved by optimizing the codebook parameters in an end-to-end next-token prediction task.

Baselines. We include BiLLM (Huang et al., 2024a), which performs effectively at the 1-bit compression level. Additionally, three more resource-intensive PTQ baselines are considered: AQLM (Egiazarian et al., 2024), which utilizes a larger number of calibration samples (4-16M tokens); QuIP# (Tseng et al., 2024) and DB-LLM (Chen et al., 2024), both of which employ model-wise distillation and a larger number of calibration samples (24-48M tokens).

Settings. ClusComp employs only 0.3M tokens for its compression. In this experiment, we further finetune the compressed LLM generated by ClusComp through end-to-end training, optimizing the codebook parameters using 16M tokens from a subset of the RedPajama dataset (Computer, 2023). This extended method is referred to as ClusComp$^+$.

Results. We report the zero-shot accuracy of ultra-low-bit LLMs in Table 3. On both Llama-2-7B and 13B, ClusComp already performs comparably to, or surpasses AQLM and QuiP#. With minimal recovery training, ClusComp$^+$ consistently outperforms these baselines on average, with the performance gap increasing for larger LLMs, indicating the robust scalability of ClusComp$^+$. On Llama-3-8B, ClusComp already exceeds all baselines, and ClusComp$^+$ further widens this margin. On Llama-3-70B, ClusComp$^+$ achieves remarkable accuracy at the 1-bit level. Furthermore, when comparing the improvements from ClusComp to ClusComp$^+$ across different Llama series, a notably larger performance gain is observed on the Llama-3 models, underscoring the effectiveness of ClusComp$^+$ on LLMs with more outliers.

4.3 Finetuning quality and efficiency

We can finetune the compressed LLMs on downstream tasks by only training the codebooks.

General-domain finetuning. We finetune the compressed LLMs on a new version of Alpaca, i.e. Alpaca-GPT4 (Peng et al., 2023), and evaluate them on both MMLU and AGIEval (Zhong et al., 2024). Here we mainly compare ClusComp to some memory-efficient finetuning methods that fully finetune the FP16 version, i.e. GaLore (Zhao et al., 2024) and LISA (Pan et al., 2024). As shown in Table 4, finetuning the compressed LLMs at the 4-bit level from ClusComp outperforms all memory-efficient finetuning methods, and rivals full finetuning. In addition, the finetuned LLMs can be used in a low bit, friendly for inference.

The superior finetuning performance can be attributed to three key advantages of ClusComp: (1) ClusComp introduces smaller compression errors; (2) Unlike QLoRA, where compressed LLMs are frozen during finetuning, ClusComp allows for the model to remain unfrozen by training the codebook parameters, enabling further mitigation of compression errors; (3) The low-rank design of

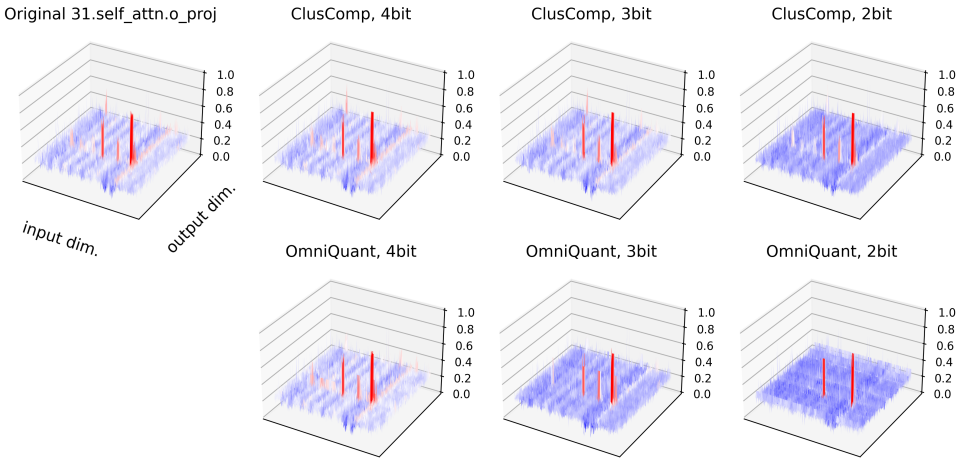

Figure 4: Weight patterns of a cherry-picked layer in Llama-2-7B. Darker red and blue indicate larger and smaller weight values, respectively. Please refer to §A.4 for the visualization setting and the visualization of more layers.

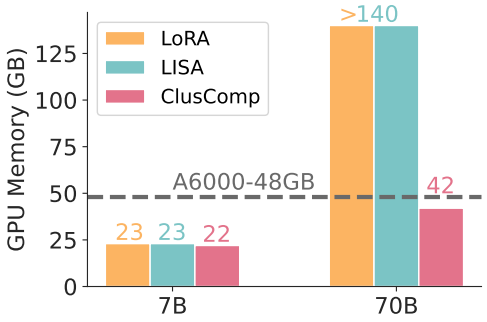

Figure 5: Memory consumption for recovery training or finetuning. 4-bit LLMs are used for ClusComp here.

LoRA limits its expressiveness. In contrast, updating the codebook in ClusComp is analogous to updating a high-rank weight matrix. In addition, the fixed-code design allows uniform training of all centroids, providing greater expressiveness and can even rival full finetuning.

4.4 Discussion

Efficiency. Figure 5 illustrates the memory efficiency of ClusComp during training, with a batch size of 1 and a sequence length of 1024. For the 70B LLM, we apply gradient checkpointing (this is not used for the 7B LLM), while omitting any additional memory-saving techniques.

Finetuning the LLM compressed by ClusComp demonstrates memory efficiency in two key ways: (1) The compressed LLM requires less memory for loading onto the GPU compared to the FP16 model; and (2) Only the codebook parameters, which contain a limited number of trainable parameters ($< 1\%$), are updated, as detailed in Table 4. Consequently, the optimizer state size remains small. ClusComp can serve not only as a model compression technique but also as an effective method for both memory-efficient and parameter-efficient finetuning.

Weight distribution. In Figure 4, we compare ClusComp's weight distribution to OmniQuant's. Notably, OmniQaunt applies uniform quantization. Overall, ClusComp's weight distribution in different bit levels can better simulate the original weight distribution, explaining ClusComp's effectiveness.

More results. Due to page limit, we recommend readers to (1) Appendix A.5 for more finetuning results with a comparison to QLoRA, LoftQ, QA-LoRA, GPTQ-LoRA and PEQA; (2) Appendix A.6 for comparing ClusComp to SqueezeLLM and AdaDim; (3) Appendix A.7 to check whether the number of clusters n or the cluster dimension g has a greater impact on the performance; and (4) Appendix A.8 for ClusComp's throughput.

5 Conclusion

The newly introduced model compression technique, ClusComp, operates by (1) independently applying clustering to the weight matrices to produce both the codebook and corresponding codes, (2) reducing compression error through block-wise knowledge distillation, and (3) enhancing model performance via efficient recovery finetuning. Comprehensive experiments demonstrate its effectiveness as a compression method at 1-4 bit levels, while also showcasing its parameter and memory efficiency for finetuning, with a competitive performance with full finetuning.

Limitations

We only evaluate ClusComp on a limited number of tasks with a total number of 7 models due to time and resource limitations. We couldn't guarantee its effectiveness on the other tasks and LLMs, and are still working on including more tasks and models to show its generalization. In addition, applying ClusComp to image generation tasks is not explored in this paper. We leave this exploration to interested readers.

ClusComp only compresses the weight matrices, while leaving the activations in FP16, which might cause OOM error for the long-context generation. However, we can combine ClusComp with activation quantization methods to address this issue.

References

Yoshua Bengio, Nicholas Léonard, and Aaron C. Courville. 2013. Estimating or propagating gradients through stochastic neurons for conditional computation. *CoRR*, abs/1308.3432.

Dan Biderman, Jose Javier Gonzalez Ortiz, Jacob Portes, Mansheej Paul, Philip Greengard, Connor Jennings, Daniel King, Sam Havens, Vitaliy Chiley, Jonathan Frankle, Cody Blakeney, and John P. Cunningham. 2024. Lora learns less and forgets less. *CoRR*, abs/2405.09673.

Yonatan Bisk, Rowan Zellers, Ronan Le Bras, Jianfeng Gao, and Yejin Choi. 2020. PIQA: reasoning about physical commonsense in natural language. In *The Thirty-Fourth AAAI Conference on Artificial Intelligence, AAAI 2020, The Thirty-Second Innovative Applications of Artificial Intelligence Conference, IAAI 2020, The Tenth AAAI Symposium on Educational Advances in Artificial Intelligence, EAAI 2020, New York, NY, USA, February 7-12, 2020*, pages 7432–7439. AAAI Press.

Yelysei Bondarenko, Markus Nagel, and Tijmen Blankevoort. 2023. Quantizable transformers: Removing outliers by helping attention heads do nothing. In *Advances in Neural Information Processing Systems 36: Annual Conference on Neural Information Processing Systems 2023, NeurIPS 2023, New Orleans, LA, USA, December 10 - 16, 2023*.

Tom B. Brown, Benjamin Mann, Nick Ryder, Melanie Subbiah, Jared Kaplan, Prafulla Dhariwal, Arvind Neelakantan, Pranav Shyam, Girish Sastry, Amanda Askell, Sandhini Agarwal, Ariel Herbert-Voss, Gretchen Krueger, Tom Henighan, Rewon Child, Aditya Ramesh, Daniel M. Ziegler, Jeffrey Wu, Clemens Winter, Christopher Hesse, Mark Chen, Eric Sigler, Mateusz Litwin, Scott Gray, Benjamin Chess, Jack Clark, Christopher Berner, Sam McCandlish, Alec Radford, Ilya Sutskever, and Dario Amodei. 2020. Language models are few-shot learners. *CoRR*, abs/2005.14165.

Jerry Chee, Yaohui Cai, Volodymyr Kuleshov, and Christopher De Sa. 2023. Quip: 2-bit quantization of large language models with guarantees. In *Advances in Neural Information Processing Systems 36: Annual Conference on Neural Information Processing Systems 2023, NeurIPS 2023, New Orleans, LA, USA, December 10 - 16, 2023*.

Hong Chen, Chengtao Lv, Liang Ding, Haotong Qin, Xiabin Zhou, Yifu Ding, Xuebo Liu, Min Zhang, Jinyang Guo, Xianglong Liu, and Dacheng Tao. 2024. DB-LLM: accurate dual-binarization for efficient llms. In *Findings of the Association for Computational Linguistics, ACL 2024, Bangkok, Thailand and virtual meeting, August 11-16, 2024*, pages 8719–8730. Association for Computational Linguistics.

Christopher Clark, Kenton Lee, Ming-Wei Chang, Tom Kwiatkowski, Michael Collins, and Kristina Toutanova. 2019. Boolq: Exploring the surprising difficulty of natural yes/no questions. In *Proceedings of the 2019 Conference of the North American Chapter of the Association for Computational Linguistics: Human Language Technologies, NAACL-HLT 2019, Minneapolis, MN, USA, June 2-7, 2019, Volume 1 (Long and Short Papers)*, pages 2924–2936. Association for Computational Linguistics.

Peter Clark, Isaac Cowhey, Oren Etzioni, Tushar Khot, Ashish Sabharwal, Carissa Schoenick, and Oyvind Tafjord. 2018. Think you have solved question answering? try arc, the AI2 reasoning challenge. *CoRR*, abs/1803.05457.

Karl Cobbe, Vineet Kosaraju, Mohammad Bavarian, Mark Chen, Heewoo Jun, Lukasz Kaiser, Matthias Plappert, Jerry Tworek, Jacob Hilton, Reiichiro Nakano, Christopher Hesse, and John Schulman. 2021. Training verifiers to solve math word problems. *CoRR*, abs/2110.14168.

Together Computer. 2023. Redpajama: An open source recipe to reproduce llama training dataset.

DeepSeek-AI, Aixin Liu, Bei Feng, Bing Xue, Bingxuan Wang, Bochao Wu, Chengda Lu, Chenggang Zhao, and et al. 2024. Deepseek-v3 technical report. *CoRR*, abs/2412.19437.

Tim Dettmers, Artidoro Pagnoni, Ari Holtzman, and Luke Zettlemoyer. 2023. Qlora: Efficient finetuning of quantized llms. In *Advances in Neural Information Processing Systems 36: Annual Conference on Neural Information Processing Systems 2023, NeurIPS 2023, New Orleans, LA, USA, December 10 - 16, 2023*.

Tim Dettmers, Ruslan Svirschevski, Vage Egiazarian, Denis Kuznedelev, Elias Frantar, Saleh Ashkboos, Alexander Borzunov, Torsten Hoefler, and Dan Alistarh. 2024. Spqr: A sparse-quantized representation for near-lossless LLM weight compression. In *The*

Twelfth International Conference on Learning Representations, ICLR 2024, Vienna, Austria, May 7-11, 2024. OpenReview.net.

Matthijs Douze, Alexandr Guzhva, Chengqi Deng, Jeff Johnson, Gergely Szilvasy, Pierre-Emmanuel Mazaré, Maria Lomeli, Lucas Hosseini, and Hervé Jégou. 2024. The faiss library. *CoRR*, abs/2401.08281.

Abhimanyu Dubey, Abhinav Jauhri, Abhinav Pandey, Abhishek Kadian, Ahmad Al-Dahle, Aiesha Letman, Akhil Mathur, Alan Schelten, Amy Yang, Angela Fan, and et al. 2024. The llama 3 herd of models. *CoRR*, abs/2407.21783.

Vage Egiazarian, Andrei Panferov, Denis Kuznedelev, Elias Frantar, Artem Babenko, and Dan Alistarh. 2024. Extreme compression of large language models via additive quantization. In *Forty-first International Conference on Machine Learning, ICML 2024, Vienna, Austria, July 21-27, 2024*. OpenReview.net.

Elias Frantar, Saleh Ashkboos, Torsten Hoefler, and Dan Alistarh. 2022. GPTQ: accurate post-training quantization for generative pre-trained transformers. *CoRR*, abs/2210.17323.

Leo Gao, Jonathan Tow, Baber Abbasi, Stella Biderman, Sid Black, Anthony DiPofi, Charles Foster, Laurence Golding, Jeffrey Hsu, Alain Le Noac'h, Haonan Li, Kyle McDonell, Niklas Muennighoff, Chris Ociepa, Jason Phang, Laria Reynolds, Hailey Schoelkopf, Aviya Skowron, Lintang Sutawika, Eric Tang, Anish Thite, Ben Wang, Kevin Wang, and Andy Zou. 2024. A framework for few-shot language model evaluation.

Dan Hendrycks, Collin Burns, Steven Basart, Andy Zou, Mantas Mazeika, Dawn Song, and Jacob Steinhardt. 2021. Measuring massive multitask language understanding. In *9th International Conference on Learning Representations, ICLR 2021, Virtual Event, Austria, May 3-7, 2021*. OpenReview.net.

Jung Hwan Heo, Jeonghoon Kim, Beomseok Kwon, Byeongwook Kim, Se Jung Kwon, and Dongsoo Lee. 2024. Rethinking channel dimensions to isolate outliers for low-bit weight quantization of large language models. In *The Twelfth International Conference on Learning Representations, ICLR 2024, Vienna, Austria, May 7-11, 2024*. OpenReview.net.

Edward J. Hu, Yelong Shen, Phillip Wallis, Zeyuan Allen-Zhu, Yuanzhi Li, Shean Wang, Lu Wang, and Weizhu Chen. 2022. Lora: Low-rank adaptation of large language models. In *The Tenth International Conference on Learning Representations, ICLR 2022, Virtual Event, April 25-29, 2022*. OpenReview.net.

Wei Huang, Yangdong Liu, Haotong Qin, Ying Li, Shiming Zhang, Xianglong Liu, Michele Magno, and Xiaojuan Qi. 2024a. Billm: Pushing the limit of post-training quantization for llms. In *Forty-first International Conference on Machine Learning, ICML 2024, Vienna, Austria, July 21-27, 2024*. OpenReview.net.

Wei Huang, Haotong Qin, Yangdong Liu, Yawei Li, Xianglong Liu, Luca Benini, Michele Magno, and Xiaojuan Qi. 2024b. Slim-llm: Salience-driven mixed-precision quantization for large language models. *CoRR*, abs/2405.14917.

Wei Huang, Xingyu Zheng, Xudong Ma, Haotong Qin, Chengtao Lv, Hong Chen, Jie Luo, Xiaojuan Qi, Xianglong Liu, and Michele Magno. 2024c. An empirical study of llama3 quantization: From llms to mllms. *Preprint*, arXiv:2404.14047.

Aniruddha Kembhavi, Mike Salvato, Eric Kolve, Min Joon Seo, Hannaneh Hajishirzi, and Ali Farhadi. 2016. A diagram is worth a dozen images. In *Computer Vision - ECCV 2016 - 14th European Conference, Amsterdam, The Netherlands, October 11-14, 2016, Proceedings, Part IV*, volume 9908 of *Lecture Notes in Computer Science*, pages 235–251. Springer.

Jeonghoon Kim, Jung Hyun Lee, Sungdong Kim, Joonsuk Park, Kang Min Yoo, Se Jung Kwon, and Dongsoo Lee. 2023. Memory-efficient fine-tuning of compressed large language models via sub-4-bit integer quantization. In *Advances in Neural Information Processing Systems 36: Annual Conference on Neural Information Processing Systems 2023, NeurIPS 2023, New Orleans, LA, USA, December 10 - 16, 2023*.

Sehoon Kim, Coleman Hooper, Amir Gholami, Zhen Dong, Xiuyu Li, Sheng Shen, Michael W. Mahoney, and Kurt Keutzer. 2024. Squeezellm: Dense-and-sparse quantization. In *Forty-first International Conference on Machine Learning, ICML 2024, Vienna, Austria, July 21-27, 2024*. OpenReview.net.

Diederik P. Kingma and Jimmy Ba. 2015. Adam: A method for stochastic optimization. In *3rd International Conference on Learning Representations, ICLR 2015, San Diego, CA, USA, May 7-9, 2015, Conference Track Proceedings*.

Diederik P. Kingma and Max Welling. 2014. Auto-encoding variational bayes. In *2nd International Conference on Learning Representations, ICLR 2014, Banff, AB, Canada, April 14-16, 2014, Conference Track Proceedings*.

Bo Li, Peiyuan Zhang, Kaichen Zhang, Fanyi Pu, Xinrun Du, Yuhao Dong, Haotian Liu, Yuanhan Zhang, Ge Zhang, Chunyuan Li, and Ziwei Liu. 2024a. Lmms-eval: Accelerating the development of large multimoal models.

Feng Li, Renrui Zhang, Hao Zhang, Yuanhan Zhang, Bo Li, Wei Li, Zejun Ma, and Chunyuan Li. 2024b. Llava-next-interleave: Tackling multi-image, video, and 3d in large multimodal models. *CoRR*, abs/2407.07895.

Yixiao Li, Yifan Yu, Chen Liang, Nikos Karampatziakis, Pengcheng He, Weizhu Chen, and Tuo Zhao. 2024c. Loftq: Lora-fine-tuning-aware quantization for large language models. In *The Twelfth International Conference on Learning Representations, ICLR 2024, Vienna, Austria, May 7-11, 2024*. OpenReview.net.

Baohao Liao and Christof Monz. 2024a. 3-in-1: 2d rotary adaptation for efficient finetuning, efficient batching and composability. *Preprint*, arXiv:2409.00119.

Baohao Liao and Christof Monz. 2024b. Apiq: Finetuning of 2-bit quantized large language model. *CoRR*, abs/2402.05147.

Ji Lin, Jiaming Tang, Haotian Tang, Shang Yang, Wei-Ming Chen, Wei-Chen Wang, Guangxuan Xiao, Xingyu Dang, Chuang Gan, and Song Han. 2024. AWQ: activation-aware weight quantization for on-device LLM compression and acceleration. In *Proceedings of the Seventh Annual Conference on Machine Learning and Systems, MLSys 2024, Santa Clara, CA, USA, May 13-16, 2024*. mlsys.org.

Yuan Liu, Haodong Duan, Yuanhan Zhang, Bo Li, Songyang Zhang, Wangbo Zhao, Yike Yuan, Jiaqi Wang, Conghui He, Ziwei Liu, Kai Chen, and Dahua Lin. 2023. Mmbench: Is your multi-modal model an all-around player? *CoRR*, abs/2307.06281.

Stuart P. Lloyd. 1982. Least squares quantization in PCM. *IEEE Trans. Inf. Theory*, 28(2):129–136.

Ilya Loshchilov and Frank Hutter. 2019. Decoupled weight decay regularization. In *7th International Conference on Learning Representations, ICLR 2019, New Orleans, LA, USA, May 6-9, 2019*. OpenReview.net.

Yuexiao Ma, Huixia Li, Xiawu Zheng, Feng Ling, Xuefeng Xiao, Rui Wang, Shilei Wen, Fei Chao, and Rongrong Ji. 2024. Affinequant: Affine transformation quantization for large language models. In *The Twelfth International Conference on Learning Representations, ICLR 2024, Vienna, Austria, May 7-11, 2024*. OpenReview.net.

Vladimir Malinovskii, Denis Mazur, Ivan Ilin, Denis Kuznedelev, Konstantin Burlachenko, Kai Yi, Dan Alistarh, and Peter Richtárik. 2024. Pv-tuning: Beyond straight-through estimation for extreme LLM compression. *CoRR*, abs/2405.14852.

Ahmed Masry, Do Xuan Long, Jia Qing Tan, Shafiq R. Joty, and Enamul Hoque. 2022. Chartqa: A benchmark for question answering about charts with visual and logical reasoning. In *Findings of the Association for Computational Linguistics: ACL 2022, Dublin, Ireland, May 22-27, 2022*, pages 2263–2279. Association for Computational Linguistics.

Minesh Mathew, Dimosthenis Karatzas, and C. V. Jawahar. 2021. Docvqa: A dataset for VQA on document images. In *IEEE Winter Conference on Applications of Computer Vision, WACV 2021, Waikoloa, HI, USA, January 3-8, 2021*, pages 2199–2208. IEEE.

Stephen Merity, Caiming Xiong, James Bradbury, and Richard Socher. 2017. Pointer sentinel mixture models. In *5th International Conference on Learning Representations, ICLR 2017, Toulon, France, April 24-26, 2017, Conference Track Proceedings*. OpenReview.net.

Rui Pan, Xiang Liu, Shizhe Diao, Renjie Pi, Jipeng Zhang, Chi Han, and Tong Zhang. 2024. LISA: layerwise importance sampling for memory-efficient large language model fine-tuning. *CoRR*, abs/2403.17919.

Yeonhong Park, Jake Hyun, SangLyul Cho, Bonggeun Sim, and Jae W. Lee. 2024. Any-precision LLM: low-cost deployment of multiple, different-sized llms. In *Forty-first International Conference on Machine Learning, ICML 2024, Vienna, Austria, July 21-27, 2024*. OpenReview.net.

Adam Paszke, Sam Gross, Soumith Chintala, Gregory Chanan, Edward Yang, Zachary DeVito, Zeming Lin, Alban Desmaison, Luca Antiga, and Adam Lerer. 2017. Automatic differentiation in pytorch. In *NIPS-W*.

Baolin Peng, Chunyuan Li, Pengcheng He, Michel Galley, and Jianfeng Gao. 2023. Instruction tuning with gpt-4. *arXiv preprint arXiv:2304.03277*.

Colin Raffel, Noam Shazeer, Adam Roberts, Katherine Lee, Sharan Narang, Michael Matena, Yanqi Zhou, Wei Li, and Peter J. Liu. 2020a. Exploring the limits of transfer learning with a unified text-to-text transformer. *J. Mach. Learn. Res.*, 21:140:1–140:67.

Colin Raffel, Noam Shazeer, Adam Roberts, Katherine Lee, Sharan Narang, Michael Matena, Yanqi Zhou, Wei Li, and Peter J. Liu. 2020b. Exploring the limits of transfer learning with a unified text-to-text transformer. *J. Mach. Learn. Res.*, 21:140:1–140:67.

Keisuke Sakaguchi, Ronan Le Bras, Chandra Bhagavatula, and Yejin Choi. 2020. Winogrande: An adversarial winograd schema challenge at scale. In *The Thirty-Fourth AAAI Conference on Artificial Intelligence, AAAI 2020, The Thirty-Second Innovative Applications of Artificial Intelligence Conference, IAAI 2020, The Tenth AAAI Symposium on Educational Advances in Artificial Intelligence, EAAI 2020, New York, NY, USA, February 7-12, 2020*, pages 8732–8740. AAAI Press.

Teven Le Scao, Angela Fan, Christopher Akiki, Ellie Pavlick, Suzana Ilic, Daniel Hesslow, Roman Castagné, Alexandra Sasha Luccioni, François Yvon, Matthias Gallé, and et al. 2022. BLOOM: A 176b-parameter open-access multilingual language model. *CoRR*, abs/2211.05100.

Wenqi Shao, Mengzhao Chen, Zhaoyang Zhang, Peng Xu, Lirui Zhao, Zhiqian Li, Kaipeng Zhang, Peng Gao, Yu Qiao, and Ping Luo. 2024. Omniquant: Omnidirectionally calibrated quantization for large language models. In *The Twelfth International Conference on Learning Representations, ICLR 2024, Vienna, Austria, May 7-11, 2024*. OpenReview.net.

Mingjie Sun, Zhuang Liu, Anna Bair, and J. Zico Kolter. 2024a. A simple and effective pruning approach for large language models. In *The Twelfth International Conference on Learning Representations, ICLR 2024, Vienna, Austria, May 7-11, 2024*. OpenReview.net.

Peize Sun, Yi Jiang, Shoufa Chen, Shilong Zhang, Bingyue Peng, Ping Luo, and Zehuan Yuan. 2024b. Autoregressive model beats diffusion: Llama for scalable image generation. *CoRR*, abs/2406.06525.

Rohan Taori, Ishaan Gulrajani, Tianyi Zhang, Yann Dubois, Xuechen Li, Carlos Guestrin, Percy Liang, and Tatsunori B. Hashimoto. 2023. Stanford alpaca: An instruction-following llama model. `https://github.com/tatsu-lab/stanford_alpaca`.

Hugo Touvron, Thibaut Lavril, Gautier Izacard, Xavier Martinet, Marie-Anne Lachaux, Timothée Lacroix, Baptiste Rozière, Naman Goyal, Eric Hambro, Faisal Azhar, Aurélien Rodriguez, Armand Joulin, Edouard Grave, and Guillaume Lample. 2023a. Llama: Open and efficient foundation language models. *CoRR*, abs/2302.13971.

Hugo Touvron, Louis Martin, Kevin Stone, Peter Albert, Amjad Almahairi, Yasmine Babaei, Nikolay Bashlykov, Soumya Batra, Prajjwal Bhargava, Shruti Bhosale, and et al. 2023b. Llama 2: Open foundation and fine-tuned chat models. *CoRR*, abs/2307.09288.

Albert Tseng, Jerry Chee, Qingyao Sun, Volodymyr Kuleshov, and Christopher De Sa. 2024. Quip#: Even better LLM quantization with hadamard incoherence and lattice codebooks. In *Forty-first International Conference on Machine Learning, ICML 2024, Vienna, Austria, July 21-27, 2024*. OpenReview.net.

Mart van Baalen, Andrey Kuzmin, Markus Nagel, Peter Couperus, Cédric Bastoul, Eric Mahurin, Tijmen Blankevoort, and Paul N. Whatmough. 2024. GPTVQ: the blessing of dimensionality for LLM quantization. *CoRR*, abs/2402.15319.

Ashish Vaswani, Noam Shazeer, Niki Parmar, Jakob Uszkoreit, Llion Jones, Aidan N. Gomez, Lukasz Kaiser, and Illia Polosukhin. 2017. Attention is all you need. In *Advances in Neural Information Processing Systems 30: Annual Conference on Neural Information Processing Systems 2017, December 4-9, 2017, Long Beach, CA, USA*, pages 5998–6008.

Yuhui Xu, Lingxi Xie, Xiaotao Gu, Xin Chen, Heng Chang, Hengheng Zhang, Zhengsu Chen, Xiaopeng Zhang, and Qi Tian. 2024a. Qa-lora: Quantization-aware low-rank adaptation of large language models. In *The Twelfth International Conference on Learning Representations, ICLR 2024, Vienna, Austria, May 7-11, 2024*. OpenReview.net.

Yuhui Xu, Lingxi Xie, Xiaotao Gu, Xin Chen, Heng Chang, Hengheng Zhang, Zhengsu Chen, Xiaopeng Zhang, and Qi Tian. 2024b. Qa-lora: Quantization-aware low-rank adaptation of large language models. In *The Twelfth International Conference on Learning Representations, ICLR 2024, Vienna, Austria, May 7-11, 2024*. OpenReview.net.

Shukang Yin, Chaoyou Fu, Sirui Zhao, Ke Li, Xing Sun, Tong Xu, and Enhong Chen. 2023. A survey on multimodal large language models. *CoRR*, abs/2306.13549.

Zhihang Yuan, Yuzhang Shang, and Zhen Dong. 2024. PB-LLM: partially binarized large language models. In *The Twelfth International Conference on Learning Representations, ICLR 2024, Vienna, Austria, May 7-11, 2024*. OpenReview.net.

Rowan Zellers, Ari Holtzman, Yonatan Bisk, Ali Farhadi, and Yejin Choi. 2019. Hellaswag: Can a machine really finish your sentence? In *Proceedings of the 57th Conference of the Association for Computational Linguistics, ACL 2019, Florence, Italy, July 28- August 2, 2019, Volume 1: Long Papers*, pages 4791–4800. Association for Computational Linguistics.

Susan Zhang, Stephen Roller, Naman Goyal, Mikel Artetxe, Moya Chen, Shuohui Chen, Christopher Dewan, Mona T. Diab, Xian Li, Xi Victoria Lin, Todor Mihaylov, Myle Ott, Sam Shleifer, Kurt Shuster, Daniel Simig, Punit Singh Koura, Anjali Sridhar, Tianlu Wang, and Luke Zettlemoyer. 2022. OPT: open pre-trained transformer language models. *CoRR*, abs/2205.01068.

Jiawei Zhao, Zhenyu Zhang, Beidi Chen, Zhangyang Wang, Anima Anandkumar, and Yuandong Tian. 2024. Galore: Memory-efficient LLM training by gradient low-rank projection. In *Forty-first International Conference on Machine Learning, ICML 2024, Vienna, Austria, July 21-27, 2024*. OpenReview.net.

Wanjun Zhong, Ruixiang Cui, Yiduo Guo, Yaobo Liang, Shuai Lu, Yanlin Wang, Amin Saied, Weizhu Chen, and Nan Duan. 2024. Agieval: A human-centric benchmark for evaluating foundation models. In *Findings of the Association for Computational Linguistics: NAACL 2024, Mexico City, Mexico, June 16-21, 2024*, pages 2299–2314. Association for Computational Linguistics.

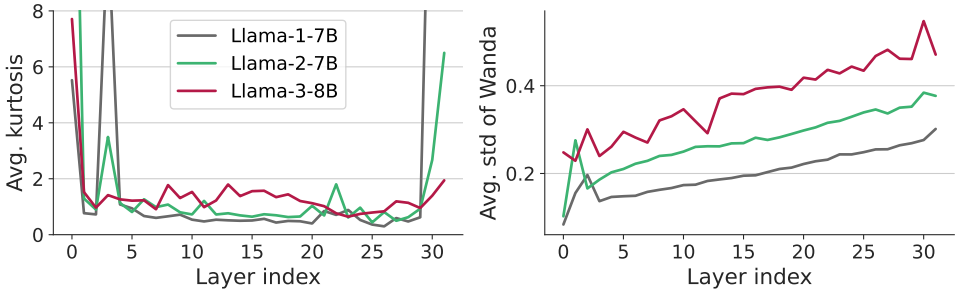

Figure A.1: From Llama-1 to Llama-3, LLMs exhibit increasing challenges for quantization. **Left:** The average kurtosis of weights across various layers in the Llama series, previously shown in Figure 2 (Right). Please refer to Figure B.1 for the kurtosis of different layer types. **Right:** The average standard deviation of the Wanda score across various layers. Please refer to Figure B.2 for the Wanda scores of different layer types. Both metrics indicate that Llama-3 has higher variance in most layers, reflecting the presence of more outliers and thus greater difficulty for quantization.

A More Results and Discussions

A.1 Quantization difficulty in Llama series

Previous works (Lin et al., 2024; Sun et al., 2024a; Heo et al., 2024) suggest that weight patterns can be identified based on activations rather than relying solely on weight magnitudes. We incorporate an additional analysis based on the Wanda score (Sun et al., 2024a) distribution to illustrate the increasing challenges of quantization in the Llama series.

Given the weight matrix $\boldsymbol{W} \in \mathbb{R}^{d_{out} \times d_{in}}$ of a linear layer and the input activations $\boldsymbol{X} \in \mathbb{R}^{NL \times d_{in}}$, where N and L represent the batch and sequence dimensions, the Wanda score $\boldsymbol{S} \in \mathbb{R}^{d_{out} \times d_{in}}$ is computed as $\boldsymbol{S}_{ij} = |\boldsymbol{W}_{ij}| \cdot ||\boldsymbol{X}_j||_2$. A smaller Wanda score within a row of $\boldsymbol{W}$ (on a per-output basis) indicates a less significant weight element.

In Figure A.1 (Right), we present the standard deviation of the Wanda scores across different layers. The results show that Llama-2 exhibits a larger standard deviation compared to Llama-1, while Llama-3 exceeds Llama-2 in this metric. A higher standard deviation reflects a more dispersed Wanda score distribution, indicating that a greater proportion of weight elements are effective and diverse. Consequently, quantization becomes more challenging, as the expanded distribution stretches the quantization grid.

A.2 Code distribution

As shown in Figure A.2, the distribution of codes after clustering is uniform. Training the codebook alone can have a similar effect as full finetuning since all weight values are updated uniformly.

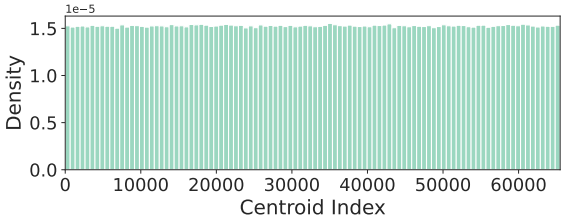

Figure A.2: Histogram of the codes.

A.3 Full results on language modeling

In Table A.1 and Table A.2, we show the full comparison across different LLMs and bit-levels on two language modeling tasks, WikiText2 and C4.

A.4 Weight visualization

To make the weight pattern more obvious, we apply these sequential processing steps: (1) take the absolute weight values; (2) downsample the grids with 8×8 maxpool kernels; (3) calculate the logarithm of these values; (4) normalize the log-values. We offer the visualization of all layers in the first and last blocks of Llama-2-7B in Figure A.3 and A.4.

A.5 More finetuning results

In-domain finetuning. We finetune Llama-2-7B on the training sets of WikiText2 and GSM8K (Cobbe et al., 2021), and report the perplexity and accuracy on their respective validation/test set. ClusComp is compared with two LoRA-based techniques: QLoRA (Dettmers et al., 2023) and LoftQ (Li et al., 2024c). As shown in Table A.6, ClusComp consistently achieves superior results with fewer bits (except at the 4-bit level on WikiText2, where it performs comparably to LoftQ), even outperforming LoRA-finetuning of the FP16 model

on GSM8K with a 2.54-bit compressed LLM.

General-domain finetuning. We finetune the compressed LLMs on Alpaca-GPT3.5 (Taori et al., 2023) and evaluate them using the MMLU benchmark (Hendrycks et al., 2021). ClusComp is compared against baseline methods that merge trained LoRA modules into the quantized linear layers after finetuning, i.e. GPTQ-LoRA, QA-LoRA (Xu et al., 2024b) and PEQA (Kim et al., 2023).

As shown in Table A.7, ClusComp consistently outperforms the baseline methods across different LLMs and bit-widths, while using fewer bits. The only exception occurs at the 4-bit level for Llama-1-7B, where ClusComp underperforms QA-LoRA by a small margin of 0.3 accuracy. The performance gap between ClusComp and baselines is enlarged for lower bits or recent LLM series.

A.6 More baselines

In this section, we compare ClusComp against SqueezeLLM (Kim et al., 2024) and AdaDim (Heo et al., 2024). As presented in Table A.8, ClusComp consistently achieves lower perplexity than SqueezeLLM, at comparable or even lower bit precision. Similarly, as shown in Table A.9, ClusComp outperforms AdaDim on both MMLU and CSR benchmarks.

A.7 Ablation study on the group size and number of clusters

We conducted experiments to determine whether the number of clusters n or the cluster dimension g has a greater impact on the performance of quantized LLMs. As shown in Table A.10, increasing n positively affects performance more than reducing g. This finding underpins our choice of $n \approx 2^{16}$. However, while n plays a crucial role in enhancing performance, selecting $n > 2^{16}$ would necessitate using 32-bit storage for the code $\boldsymbol{q}$, substantially increasing the bits-per-parameter and adversely affecting memory efficiency. Therefore, we always choose $n < 2^{16}$.

A.8 Throughput

Originally, the data type of the codebook $\boldsymbol{C}$ is in 16-bit, which facilitates our following recovery training and finetuning step. However, if the codebook can be further quantized, we have two additional advantages: (1) The model size can be slightly reduced (Only slightly since the majority of bits is allocated to the code $\boldsymbol{q}$.); (2) The inference can speed up, since the codebook becomes smaller. In sum, we can keep the codebook in 16-bit if we want to do the recovery training or finetuning. If we are only interested in inference, we can further quantize the codebook to a lower bit level.

As shown in Table A.11, the performance doesn't change if we quantize the codebook from 16-bit to 8-bit. When quantizing the codebook to 4-bit, the perplexity slightly increases, but is still comparable to the best baseline at the 4-bit level and outperforms the best baseline at the 2-bit level. However, if we further quantize the codebook to the 2-bit level, the perplexity increases significantly. Therefore, we can safely quantize the codebook to 8-bit or 4-bit.

In Table A.12, we show the throughput of ClusComp. When the codebook stays in the FP16 format, the throughput is only slightly better than the FP16 LLM, because non-uniform compression is not friendly to hardware. To enhance the inference, we can further quantize the codebook to a lower bit level. When the codebook is quantized to a 4-bit level, we can roughly achieve a 2× speedup.

A.9 Compression performance of the multimodal backbone

In Table A.13, we show the performance of the compressed Llama-3-8B backbone in LLaVA-Next-8B. ClusComp again shows its superior performance.

B Experimental Details

B.1 Clustering

We use the K-means implementation from the Faiss library (Douze et al., 2024). The number of iterations is set to 20, with all default settings for other arguments.

B.2 Block-wise error minimization

For all LLMs, 128 calibration sentences with a length of 2048 tokens are randomly selected from the WikiText-2 training set (Merity et al., 2017). The detailed hyper-parameters are listed in Table B.1. Only the codebooks are trained while keeping all other parameters (from the embedding layer, output layer and normalization layers) frozen.

B.3 Recovery training

For the recovery training, we randomly sample 1024 sentences with a length of 4096 tokens from

a subset of RedPajama (Computer, 2023)[4]. Then we train the compressed LLMs to predict the next token by only tuning the codebook parameters. The hyperparameters used in this step are listed in Table B.1.

B.4 In-domain finetuning

We follow the settings from (Li et al., 2024c), and finetune the compressed LLM on the training set of WikiText2 and on the training set of GSM8K. The hyperparameters for finetuning are listed in Table B.2. We evaluate the finetuned model on the validation set of WikiText2 and on the test set of GSM8K every epoch and report the best perplexity or accuracy.

B.5 General-domain finetuning

The finetuning hyper-parameters are listed in Table B.2, which is similar to the ones in QA-LoRA (Xu et al., 2024b) on Alpaca-GPT3.5, or to the ones in LISA (Pan et al., 2024) on Alpaca-GPT4.

[4] https://huggingface.co/datasets/togethercomputer/RedPajama-Data-1T-Sample

Method	Setting	#Bit	1-7B	2-7B	2-13B	2-70B	3-8B	3-70B
-	-	16.00	5.68	5.47	4.88	3.31	6.12	2.90
RTN	w4g128	4.13	5.96	5.72	4.98	3.46	8.50	3.60
GPTQ	w4g128	4.13	5.85	5.61	4.98	3.42	6.50	3.30
AWQ	w4g128	4.13	5.81	5.62	4.97	-	6.60	3.30
GPTVQ	w4g128	4.13	-	5.68	4.97	**3.39**	-	-
AffineQuant	w4g128	4.13	5.77	5.58	4.95	-	-	-
OmniQuant	w4g128	4.16	5.77	5.58	4.95	3.40	-	-
ClusComp$^-$	g4n65500	≤4.14	5.88 (4.14)	5.67 (4.14)	5.04 (4.09)	3.44 (4.03)	6.59 (4.13)	3.28 (4.03)
ClusComp	g4n65500	≤4.14	**5.73** (4.14)	**5.54** (4.14)	**4.94** (4.09)	3.40 (4.03)	**6.39** (4.13)	**3.12** (4.03)
RTN	w4	4.00	6.43	6.11	5.20	3.67	8.70	-
GPTQ	w4	4.00	6.13	5.83	5.13	3.58	**7.00**	-
AWQ	w4	4.00	6.08	6.15	5.12	-	7.10	-
QuIP	w4	4.00	-	-	-	3.53	-	-
AffineQuant	w4	4.00	**5.84**	5.69	**5.01**	-	-	-
OmniQuant	w4	4.00	5.86	5.74	5.02	**3.47**	-	-
ClusComp$^-$	g5n65500	**3.38**	6.27	5.90	-	-	-	-
ClusComp	g5n65500	**3.38**	**5.84**	**5.67**	-	-	-	-
RTN	w3g128	3.13	7.01	6.66	5.51	3.97	27.91	11.84
GPTQ	w3g128	3.13	6.55	6.29	5.42	3.85	8.22	5.22
AWQ	w3g128	3.13	6.46	6.24	5.32	-	**8.19**	**4.81**
SliM-LLM$^+$	w3g128	3.13	**6.07**	5.94	5.11	**3.35**	-	-
AffineQuant	w3g128	3.13	6.14	6.08	5.28	-	-	-
GPTVQ	w3g128	3.13	-	**5.82**	**5.10**	3.55	-	-
OmniQuant	w3g128	3.15	6.15	6.03	5.28	3.78	-	-
RTN	w3	3.00	25.73	5.4e2	10.68	7.52	2.2e3	-
GPTQ	w3	3.00	8.06	8.37	6.44	4.82	13.0	-
AWQ	w3	3.00	11.88	24.00	10.45	-	12.8	-
QuIP	w3	3.00	-	-	-	3.85	7.5	-
AffineQuant	w3	3.00	6.30	6.55	5.62	-	-	-
OmniQuant	w3	3.00	6.49	6.58	5.58	3.92	-	-
ClusComp$^-$	g6n65500	≤2.89	6.74 (2.89)	6.54 (2.89)	6.27 (2.81)	4.02 (2.72)	8.77 (2.87)	4.98 (2.72)
ClusComp	g6n65500	≤**2.89**	**6.01** (2.89)	**5.86** (2.89)	**5.18** (2.81)	**3.72** (2.72)	**7.34** (2.87)	**4.63** (2.72)
ClusComp$^-$	g7n65500	2.54	7.79	7.64	-	-	-	-
ClusComp	g7n65500	2.54	**6.28**	**6.15**	-	-	-	-
RTN	w2g64	2.25	1.9e2	4.3e2	26.22	10.31	-	-
GPTQ	w2g64	2.25	22.10	20.85	22.44	NAN	1.8e2	-
AWQ	w2g64	2.25	2.5e5	2.1e5	1.2e5	-	-	-
GPTVQ	w2g64	2.25	-	7.22	6.08	**4.39**	-	-
AffineQuant	w2g64	2.25	8.35	9.05	7.11	-	-	-
OmniQuant	w2g64	2.28	8.90	9.62	7.56	6.11	-	-
ClusComp$^-$	g8n65500	≤2.29	10.25 (2.29)	11.10 (2.29)	14.39 (2.19)	-	29.20 (2.27)	-
ClusComp	g8n65500	≤2.29	**6.66** (2.29)	**6.61** (2.29)	**5.74** (2.19)	-	**9.68** (2.27)	-
RTN	w2g128	2.13	1.9e3	4.2e3	1.2e2	27.27	1.9e3	4.6e5
GPTQ	w2g128	2.13	44.01	36.77	28.14	NAN	2.1e2	11.9
AWQ	w2g128	2.13	2.6e5	2.2e5	1.2e5	-	1.7e6	1.7e6
SliM-LLM$^+$	w2g128	2.13	9.68	10.87	7.59	6.44	-	-
QuIP	w2g128	2.13	-	39.73	13.48	6.64	84.97	13.03
PB-LLM	w2g128	2.13	-	25.37	49.81	NAN	44.12	11.68
GPTVQ	w2g128	2.13	-	8.23	6.50	4.64	-	-
AffineQuant	w2g128	2.13	13.51	10.87	7.64	-	-	
OmniQuant	w2g128	2.14	9.72	11.06	8.26	6.55	-	-
ClusComp$^-$	g8	≤2.15	28.76	21.9	14.50	5.43	2.1e2	11.40
ClusComp	g8	≤2.15	**7.06** (2.15,n35000)	**7.04** (2.15,n35000)	**5.85** (2.14,n50000)	**4.37** (2.07,n65500)	**11.57** (2.14,n35000)	**7.61** (2.07,n65500)
ClusComp$^-$	g9n65500	2.11	-	22.71	-	-	-	-
ClusComp	g9n65500	2.11	-	**7.12**	-	-	-	-
RTN	w2	2.00	1.1e5	3.8e4	5.6e4	2.0e4	2.7e6	-
GPTQ	w2	2.00	2.1e3	7.7e3	2.1e3	77.95	5.7e4	-
QuIP	w2	2.00	-	-	-	6.33	85.1	-
AffineQuant	w2	2.00	9.53	35.07	12.42	-	-	-
OmniQuant	w2	2.00	15.47	37.37	17.21	7.81	-	-
ClusComp$^-$	g9	≤2.01	65.09	52.38	22.90	9.84	3.1e2	-
ClusComp	g9	≤2.01	**7.49** (2.00,n45000)	**7.50** (2.00,n45000)	**6.17** (1.99,n65500)	**4.83** (1.85,n65500)	**12.33** (2.01,n50000)	-

Table A.1: The full perplexity results of Llama series on WikiText2. "g" and "n" denote the dimension and number of centroids in the codebook, respectively. The number in the brackets is the exact bits of different settings for different LLMs.

Method	Setting	#Bit	1-7B	2-7B	2-13B	2-70B	3-8B	3-70B
-	-	16.00	7.08	6.97	6.46	5.52	9.20	5.87
RTN	w4g128	4.13	7.37	7.24	6.58	5.63	13.40	8.90
GPTQ	w4g128	4.13	7.21	7.12	6.56	**5.58**	10.40	**6.94**
AWQ	w4g128	4.13	7.21	7.13	6.56	-	9.40	7.00
AffineQuant	w4g128	4.13	7.20	7.12	6.56	-	-	-
OmniQuant	w4g128	4.16	7.21	7.12	6.56	**5.58**	-	-
ClusComp$^-$	g4n65500	$\leq$4.14	7.27 (4.14)	7.16 (4.14)	6.63 (4.09)	5.61 (4.03)	9.39 (4.13)	7.02 (4.03)
ClusComp	g4n65500	$\leq$4.13	**7.17** (4.14)	**7.09** (4.14)	**6.55** (4.09)	5.61 (4.03)	**9.27** (4.13)	6.99 (4.03)
RTN	w3	3.00	28.26	4.0e2	12.51	10.02	2.2e3	-
GPTQ	w3	3.00	9.49	9.81	8.02	6.57	13.0	-
AWQ	w3	3.00	13.26	23.85	13.07	-	12.8	-
QuIP	w3	3.00	-	-	-	6.14	-	-
AffineQuant	w3	3.00	8.03	8.57	7.56	-	-	-
OmniQuant	w3	3.00	8.19	8.65	7.44	6.06	-	-
ClusComp$^-$	g6n65500	$\leq$2.89	8.14 (2.89)	8.19 (2.89)	8.21 (2.81)	6.06 (2.72)	12.41 (2.87)	8.26 (2.72)
ClusComp	g6n65500	$\leq$**2.89**	**7.64** (2.89)	**7.61** (2.89)	**6.91** (2.81)	**5.86** (2.72)	**11.31** (2.87)	**8.26** (2.72)
ClusComp$^-$	g7n65500	2.54	9.46	9.51	-	-	-	-
ClusComp	g7n65500	2.54	**8.10**	**8.13**	-	-	-	-
RTN	w2g64	2.25	1.5e2	4.8e2	28.69	13.43	-	-
GPTQ	w2g64	2.25	17.71	19.40	12.48	NAN	-	-
AWQ	w2g64	2.25	2.8e5	1.6e5	9.5e4	-	-	-
OmniQuant	w2g64	2.28	11.78	12.72	10.05	7.88	-	-
ClusComp$^-$	g8n65500	$\leq$2.29	13.06 (2.29)	14.07 (2.29)	19.75 (2.19)	-	38.68 (2.27)	-
ClusComp	g8n65500	$\leq$2.29	**8.76** (2.29)	**8.88** (2.29)	**7.75** (2.19)	-	**15.57** (2.27)	-
RTN	w2g128	2.13	1.0e3	4.9e3	1.4e2	42.13	1.9e3	-
GPTQ	w2g128	2.13	27.71	33.70	20.97	NAN	2.1e2	-
AWQ	w2g128	2.13	1.9e5	1.7e5	9.4e4	-	1.7e6	-
SliM-LLM$^+$	w2g128	2.13	14.99	18.18	10.24	8.40	-	-
QuIP	w2g128	2.13	-	31.94	16.16	8.17	1.3e2	22.24
PB-LLM	w2g128	2.13	-	29.84	19.82	8.95	79.21	33.91
AffineQuant	w2g128	2.13	-	16.02	10.98	-	-	-
OmniQuant	w2g128	2.14	12.97	15.02	11.05	8.52	-	-
ClusComp$^-$	g8	$\leq$2.15	29.67	25.26	18.83	7.59	1.9e2	16.52
ClusComp	g8	$\leq$2.15	**9.33** (2.15,n35000)	**9.49** (2.15,n35000)	**7.92** (2.14,n50000)	**6.44** (2.07,n65500)	**17.89** (2.14,n35000)	**10.81** (2.07,n65500)
ClusComp$^-$	g9n65500	2.11	-	27.37	-	-	-	-
ClusComp	g9n65500	2.11	-	**9.73**	-	-	-	-
RTN	w2	2.00	1.3e5	4.8e4	7.2e4	2.4e4	2.7e6	-
GPTQ	w2	2.00	6.9e2	NAN	3.2e2	48.82	5.7e4	-
QuIP	w2	2.00	-	-	-	-	1.3e2	-
OmniQuant	w2	2.00	24.89	90.64	26.76	12.28	8.2e5	
ClusComp$^-$	g9	$\leq$2.01	74.61	50.08	24.47	13.96	2.2e2	-
ClusComp	g9	$\leq$2.01	**10.11** (2.00,n45000)	**10.29** (2.00,n45000)	**8.49** (1.99,n65500)	**7.02** (1.85,n65500)	**21.45** (2.01,n50000)	-

Table A.2: The full perplexity results of Llama series on C4. "g" and "n" denote the dimension and number of centroids in the codebook, respectively. The number in the brackets is the exact bits of different settings for different LLMs.

Method	#Bit	PIQA		ARC-e		ARC-c		BoolQ	HellaSwag		WinoGrande	Avg
		acc	**acc_n**	acc	**acc_n**	acc	**acc_n**	**acc**	acc	**acc_n**	**acc**	
Llama-2-7B	16.00	-	79.1	-	74.6	-	46.3	77.7	-	76.0	69.1	70.5
ClusComp	4.14	77.5	79.2	75.3	72.8	42.7	45.3	76.2	56.5	75.1	68.9	69.6
RTN	3.13	-	76.8	-	70.5	-	42.9	71.7	-	**74.0**	67.6	67.3
GPTQ	3.13	-	77.4	-	68.1	-	40.7	71.0	-	72.5	67.3	66.2
GPTVQ	3.13	-	**77.6**	-	**72.7**	-	**43.7**	71.7	-	72.7	67.6	67.7
ClusComp	**2.89**	76.8	**77.6**	74.4	71.3	42.3	42.9	**74.6**	54.4	72.4	**68.8**	**67.9**
RTN	2.25	-	58.8	-	36.7	-	24.8	41.9	-	40.4	51.9	42.4
GPTQ	2.25	-	60.8	-	39.0	-	25.2	59.3	-	45.8	55.5	47.6
GPTVQ	2.25	-	73.3	-	63.4	-	35.9	66.3	-	63.9	**66.1**	61.5
ClusComp	2.29	74.9	**76.0**	69.8	**65.2**	37.7	**37.4**	**73.0**	51.1	**68.4**	65.0	**64.1**
ClusComp	2.15	74.3	75.1	69.6	65.2	35.7	38.4	69.5	49.2	66.4	63.5	63.0
RTN	2.13	-	51.1	-	28.0	-	25.0	41.1	-	26.6	49.9	36.9
GPTQ	2.13	-	54.8	-	30.6	-	25.1	53.4	-	33.1	51.5	41.4
GPTVQ	2.13	-	70.7	-	58.1	-	31.5	63.7	-	58.5	60.9	57.2
ClusComp	**2.00**	72.6	**73.7**	67.0	**62.8**	32.9	**36.6**	**70.9**	47.2	**63.5**	**63.4**	**61.8**
Llama-2-13B	16.00	-	80.5	-	77.5	-	49.2	80.5	-	79.4	72.1	73.2
ClusComp	4.09	78.9	79.9	78.9	76.9	47.7	49.2	81.4	60.0	79.0	72.4	73.1
RTN	3.13	-	78.9	-	74.3	-	46.8	77.3	-	76.5	70.8	70.8
GPTQ	3.13	-	79.3	-	75.8	-	47.0	78.9	-	**77.2**	70.4	71.4
GPTVQ	3.13	-	79.4	-	75.3	-	**48.1**	79.0	-	77.0	**71.7**	71.8
ClusComp	**2.81**	78.7	**79.7**	78.5	**76.7**	45.9	47.8	**80.7**	58.3	76.8	71.4	**72.2**
RTN	2.25	-	61.6	-	41.6	-	25.4	49.8	-	48.2	51.9	46.4
GPTQ	2.25	-	70.1	-	56.7	-	31.6	51.1	-	56.6	58.9	54.2
GPTVQ	2.25	-	76.2	-	71.9	-	43.3	67.6	-	70.0	68.2	66.2
ClusComp	2.19	76.6	**77.3**	75.0	**72.9**	40.8	**43.9**	**78.1**	55.3	**73.3**	**68.4**	**69.0**
ClusComp	2.14	76.7	77.1	73.5	71.6	39.9	42.8	77.5	54.6	73.1	68.0	68.4
RTN	2.13	-	58.4	-	32.3	-	25.5	47.9	-	39.4	48.9	42.1
GPTQ	2.13	-	59.5	-	40.2	-	27.7	57.1	-	41.6	53.4	46.6
GPTVQ	2.13	-	75.2	-	68.3	-	39.5	70.7	-	65.7	**67.5**	64.5
ClusComp	**1.99**	75.6	**77.7**	74.7	**73.6**	39.9	**42.1**	**74.0**	53.0	**71.0**	67.1	**67.6**

Table A.3: Zero-shot evaluation of the quantized Llama-2-7B and Llama-2-13B, with baseline results taken from van Baalen et al. (2024). "acc" and "acc_n" mean accuracy and normalized accuracy, respectively. We offer the results of all metrics for a convenient comparison of the follow-up works. But only the highlighted **metrics** are used to calculate the average accuracy.

Method	#Bit	PIQA		ARC-e		ARC-c		BoolQ	HellaSwag		WinoGrande	Avg
		acc	acc_n	**acc**	acc_n	**acc**	acc_n	acc	**acc**	acc_n	**acc**	
Llama-3-8B	16.00	79.9	-	80.1	-	50.4	-	-	60.2	-	72.8	68.6
RTN	4.13	76.6	-	70.1	-	45.0	-	-	56.8	-	71.0	63.9
GPTQ	4.13	78.4	-	78.8	-	47.7	-	-	59.0	-	72.6	67.3
AWQ	4.13	**79.1**	-	79.7	-	49.3	-	-	59.1	-	**74.0**	68.2
SliM-LLM	4.13	78.9	-	79.9	-	49.4	-	-	58.7	-	72.6	67.9
ClusComp	4.13	**79.1**	80.5	**80.9**	79.6	**49.7**	54.1	81.1	**59.3**	78.3	72.9	**68.4**
RTN	3.13	62.3	-	32.1	-	22.5	-	-	29.1	-	54.7	40.2
GPTQ	3.13	74.9	-	70.5	-	37.7	-	-	54.3	-	71.1	61.7
AWQ	3.13	77.7	-	74.0	-	43.2	-	-	55.1	-	72.1	64.4
SliM-LLM	3.13	**77.8**	-	73.7	-	42.9	-	-	55.5	-	**72.8**	64.5
RTN	3.00	56.2	-	31.1	-	20.0	-	-	27.5	-	53.1	35.6
GPTQ	3.00	60.8	-	38.8	-	22.3	-	-	41.8	-	60.9	44.9
AWQ	3.00	71.9	-	66.7	-	35.1	-	-	50.7	-	64.7	57.8
QuIP	3.00	76.8	-	72.9	-	41.0	-	-	55.4	-	72.5	63.7
ClusComp	**2.87**	77.7	78.8	**76.0**	74.5	**43.9**	47.6	79.0	**56.0**	74.6	71.0	**64.9**
ClusComp	2.27	70.6	71.8	63.5	57.4	31.4	35.5	74.7	49.6	66.1	67.1	56.4
RTN	2.13	53.1	-	24.8	-	22.1	-	-	26.9	-	53.1	36.0
GPTQ	2.13	53.9	-	28.8	-	19.9	-	-	27.7	-	50.5	36.2
AWQ	2.13	52.4	-	24.2	-	21.5	-	-	25.6	-	50.7	34.9
SliM-LLM	2.13	57.1	-	35.4	-	26.1	-	-	28.9	-	56.6	40.8
PB-LLM	2.13	57.0	-	37.8	-	17.2	-	-	29.8	-	52.5	38.8
ClusComp	2.14	**68.0**	67.1	**54.7**	49.0	**26.4**	28.8	71.5	**47.0**	63.0	**62.4**	**51.7**
RTN	2.00	53.1	-	24.7	-	21.9	-	-	25.6	-	51.1	35.3
GPTQ	2.00	52.8	-	25.0	-	20.5	-	-	26.6	-	49.6	34.9
AWQ	2.00	55.2	-	25.2	-	21.3	-	-	25.4	-	50.4	35.5
QuIP	2.00	52.9	-	29.0	-	21.3	-	-	29.2	-	51.7	36.8
ClusComp	2.01	**70.1**	69.6	**63.3**	57.7	**31.9**	34.2	66.6	**44.4**	58.0	**58.4**	**53.6**

Table A.4: Zero-shot evaluation of the quantized Llama-3-8B, with baseline results taken from (Huang et al., 2024c). "acc" and "acc_n" mean accuracy and normalized accuracy, respectively. We offer the results of all metrics for a convenient comparison of the follow-up works. But only the highlighted **metrics** (excluding BoolQ) are used to calculate the average accuracy.

Method	#Bit	PIQA	ArcE	ArcC	Hella.	Wino.	Avg
Llama-2-7B	16.00	78.1	76.3	43.4	57.1	69.1	64.8
QuIP#	2.02	**75.1**	64.6	**34.6**	48.3	64.9	57.5
AQLM	2.02	73.6	61.9	33.3	**49.5**	64.2	56.5
ClusComp	2.00	72.6	67.0	32.9	47.2	63.4	56.6
ClusComp$^+$	2.00	73.5	**67.2**	33.9	49.3	**65.1**	**57.8**
Llama-2-13B	16.00	79.1	79.4	48.4	60.0	72.2	67.8
QuIP#	2.01	**77.3**	69.3	39.5	53.4	67.7	61.5
AQLM	1.97	76.2	69.8	37.8	53.7	65.4	60.6
ClusComp	1.99	75.6	74.7	39.9	53.0	67.1	62.0
ClusComp$^+$	1.99	76.8	**74.9**	**40.7**	**54.5**	**68.4**	**63.1**
Llama-3-8B	16.00	79.7	80.1	50.4	60.2	72.6	68.6
QuiP	2.00	52.9	29.0	21.3	29.2	51.7	36.8
PB-LLM	2.00	57.0	37.8	17.2	29.8	52.5	38.8
DB-LLM	2.00	68.9	59.1	28.2	42.1	60.4	51.8
ClusComp	2.01	70.1	63.3	31.9	44.4	58.4	53.6
ClusComp$^+$	2.01	**74.8**	**66.7**	**34.8**	**49.6**	**63.4**	**57.8**
Llama-3-70B	16.00	82.5	86.7	60.4	66.3	80.9	75.4
QuIP	2.00	65.3	48.9	26.5	40.9	**61.7**	48.7
PB-LLM	1.70	56.5	49.9	25.8	34.9	53.1	44.1
BiLLM	1.10	58.2	46.4	25.1	37.5	53.6	44.2
ClusComp	1.14	56.9	32.5	20.6	32.3	51.6	39.7
ClusComp$^+$	1.14	**69.5**	**57.2**	**30.1**	**44.2**	56.0	**51.4**

Table A.5: Zero-shot accuracy on ultra-low-bit LLMs.

Method	#Bit	WikiText2 PPL ↓	GSM8K Acc ↑
LoRA	16.00	5.08	36.9
QLoRA	4.25 + 0.40	5.70	35.1
LoftQ	4.25 + 0.40	**5.24**	35.0
ClusComp	**4.15**	5.26	**41.0**
QLoRA	3.25 + 0.40	5.73	32.1
LoftQ	3.25 + 0.40	5.63	32.9
ClusComp	**3.38**	**5.37**	**39.9**
QLoRA	2.25 + 0.40	NAN	NAN
LoftQ	2.25 + 0.40	7.85	20.9
ClusComp	2.54	**5.78**	**37.2**
ClusComp	**2.29**	6.10	36.0

Table A.6: In-domain finetuning performance on Llama-2-7B. Two bits are shown for baselines since the LoRA modules aren't merged to the quantized LLMs. The first and second numbers denote the quantized LLM and the converted bits from LoRA modules.

Method	#Bit	MMLU (0-shot, Acc ↑)					MMLU (5-shot, Acc ↑)				
		Hums.	STEM	Social	Other	Avg	Hums.	STEM	Social	Other	Avg
Llama-1-7B	16.00	32.4	26.6	31.4	37.2	32.1	33.3	29.8	37.8	38.0	34.6
GPTQ-LoRA	4.50	35.7	30.9	38.0	44.0	37.1	33.8	31.3	37.4	42.2	36.0
QA-LoRA	4.50	**36.9**	**31.4**	**40.3**	**44.9**	**38.3**	36.6	32.4	**44.8**	**44.9**	**39.4**
PEQA	**4.00**	-	-	-	-	-	34.9	28.9	37.5	40.1	34.8
ClusComp	4.15	**36.9**	**31.4**	40.0	44.2	38.0	**36.8**	**34.1**	42.7	43.9	39.1
GPTQ-LoRA	3.50	31.5	28.9	31.8	36.8	32.2	31.6	30.1	35.6	39.8	34.0
QA-LoRA	3.50	36.0	**34.1**	**42.0**	42.3	38.3	35.6	30.5	**41.5**	42.7	37.4
ClusComp	**3.38**	**38.2**	32.7	41.2	**45.4**	**39.2**	**36.3**	**31.4**	41.3	**43.0**	**37.8**
GPTQ-LoRA	2.50	24.1	22.1	22.5	23.7	23.2	23.4	26.2	26.4	28.4	25.8
QA-LoRA	2.50	26.4	25.5	25.6	28.7	26.5	27.3	26.1	26.1	30.3	27.5
ClusComp	**2.29**	**32.6**	**29.7**	**34.4**	**37.0**	**33.3**	**31.1**	**30.1**	**37.8**	**37.2**	**33.7**
Llama-2-7B	16.00	38.9	32.9	46.6	44.9	40.7	43.0	36.4	51.4	52.2	45.5
QA-LoRA	4.50	41.1	35.4	50.2	50.1	43.9	42.1	34.4	49.1	50.3	43.9
ClusComp	**4.15**	**41.6**	**36.3**	**52.3**	**51.1**	**44.9**	**42.8**	**38.1**	**52.2**	**53.1**	**46.1**
Llama-2-13B	16.00	48.1	42.7	60.5	59.5	52.3	53.3	44.1	63.3	61.0	55.3
QA-LoRA	4.50	48.2	41.7	60.4	58.7	51.9	48.0	43.0	59.7	57.4	51.7
ClusComp	**4.09**	**49.2**	**42.9**	**61.6**	**60.2**	**52.9**	**52.4**	**43.2**	**62.9**	**61.6**	**54.7**

Table A.7: General-domain finetuning performance, with baseline results from Xu et al. (2024b).

Method	#Bit	Llama-2-7B	Llama-2-13B	Llama-2-70B
-	16.00	5.47	4.88	3.31
SqueezeLLM	4.27	5.57	4.96	-
ClusComp	$\leq$ **4.14**	**5.54** (4.14)	**4.94** (4.09)	-
SqueezeLLM	3.02	6.18	5.36	3.77
ClusComp	$\leq$ **2.89**	**5.86** (2.89)	**5.18** (2.81)	**3.72** (2.72)
SqueezeLLM	2.22	10.79	7.91	4.99
SqueezeLLM	2.05	13.64	8.56	5.38
SqueezeLLM	2.01	35.49	41.02	9.44
ClusComp	$\leq$ 2.00	**7.50** (2.00)	**6.17** (1.99)	**4.83** (1.85)

Table A.8: The perplexity of Llama-2 on WikiText2. The values in the brackets are the exact bits of ClusComp for different LLMs. The SqueezeLLM results are taken from Kim et al. (2024).

Method	#Bit	Llama-2-7B		Llama-2-13B	
		MMLU (5-shot ↑)	**CSR** (0-shot ↑)	**MMLU** (5-shot ↑)	**CSR** (0-shot ↑)
-	16.00	46.0	67.9	55.6	70.3
GPTQ-AdaDim	4.13	45.3	67.7	54.6	70.1
ClusComp	$\leq$ 4.14	**45.6**	**68.2**	**55.1**	**70.8**
GPTQ-AdaDim	3.13	41.3	66.4	**52.3**	68.7
ClusComp	$\leq$ **2.89**	**43.2**	**67.2**	**52.3**	**69.5**

Table A.9: The accuracy of quantized LLMs on MMLU and four commonsense reasoning (CSR) tasks (PIQA, HellaSwag, WinoGrande and ARC-easy). Following AdaDim, we use lm-eval v0.3.0 (Gao et al., 2024) for the evaluation. The GPTQ-AdaDim results are taken from Heo et al. (2024).

Setting	#Bit	Wiki2
g4	4.14	**5.67**
g5	3.38	5.90
g6	2.89	6.54
g7	2.54	7.64
g8	2.29	11.10

(a) $n = 65500$. Perplexity changes smoothly.

Setting	#Bit	Wiki2
g7n16384	2.35	**23.14**
g7n4096	2.30	9.4e2
g8n65500	2.29	**11.10**
g8n50000	2.15	21.90
g8n4096	2.02	5.4e3

(b) Same g. Perplexity changes dramatically.

Setting	#Bit	Wiki2
g7n16384	2.35	23.14
g7n4096	2.30	9.4e2
g8n65500	2.29	**11.10**

(c) Same g. Perplexity changes dramatically.

Table A.10: Ablation study of ClusComp$^-$ on the number of clusters n and the cluster dimension g in the codebook reveals that n plays a more significant role in the performance of the quantized LLM. **(a)** The perplexity remains relatively stable with variations in g, although changes in g lead to substantial differences in the bit requirement, as most bits are used to store the codes $\boldsymbol{q}$. Specifically, smaller g values result in larger $\boldsymbol{q}$. Refer to Table 1 for detailed examples. **(b)** In contrast, perplexity is highly sensitive to changes in n. Adjusting n causes only a minor change in the bit requirement, as storing the codebook is memory-efficient. **(c)** For comparable bit budgets, n has a greater impact on performance than g.

Method	Bit for codebook	Avg. Bit	2-7B	2-70B	3-8B	3-70B
-	-	16.00	5.47	3.31	6.12	2.90
Best baseline	-	4.13	5.58	3.39	6.50	3.30
ClusComp	16	$\leq$ 4.14	5.54 (4.14)	3.40 (4.03)	6.39 (4.13)	3.12 (4.03)
ClusComp	8	$\leq$ 4.11	5.54 (4.11)	3.40 (4.03)	6.39 (4.10)	3.13 (4.03)
ClusComp	4	$\leq$ 4.07	5.59 (4.07)	3.43 (4.02)	6.52 (4.07)	3.26 (4.02)
ClusComp	2	$\leq$ 4.05	25.44 (4.05)	5.64 (4.01)	1.2e5 (4.05)	96.52 (4.01)
Best baseline	-	$\leq$ 2.13	35.07 (2.00)	4.64 (2.13)	85.10 (2.00)	11.68 (2.13)
ClusComp	16	$\leq$ 2.07	7.50 (2.00)	4.37 (2.07)	12.33 (2.01)	7.61 (2.07)
ClusComp	8	$\leq$ 2.04	7.50 (1.92)	4.37 (2.04)	12.33 (1.92)	7.63 (2.04)
ClusComp	4	$\leq$ 2.03	7.63 (1.86)	4.42 (2.03)	12.77 (1.86)	7.64 (2.03)
ClusComp	2	$\leq$ 2.02	6.5e3 (1.83)	21.07 (2.02)	1.7e5 (1.83)	2.3e4 (2.02)

Table A.11: The perplexity of ClusComp with quantized codebook on WikiText2. The results of the best baseline are taken from Table A.1. The values in the brackets are the exact bits for different LLMs. We can observe: (1) 8-bit codebook offers the same perplexity as 16-bit's; (2) 4-bit codebook slightly hurts the performance, but is still comparable to the best baseline at the 4-bit level and outperforms the best baseline at the 2-bit level. (3) The results of the 2-bit codebook are not acceptable.

#Bits for Codebook	Avg. #Bit	Llama-2-7B	Llama-2-70B
-	16.00	1.00×	1.00×
16.00	2.01	1.29×	1.17×
8.00	1.92	1.31×	1.19×
4.00	1.86	2.10×	1.81×

Table A.12: Throughput comparison between ClusComp and the FP16 version. Originally, the codebook in ClusComp remained in FP16. For further inference speedup, we can uniformly quantize it to a lower bit level.

Method	Setting	Bit	WikiText2 ↓	C4 ↓	PTB ↓
-	-	16.00	9.5	14.8	16.3
GPTQ	w4g128	4.13	**9.5**	14.8	17.1
AWQ	w4g128	4.13	9.9	15.3	**16.9**
ClusComp$^-$	s4n65500	4.13	9.9	**13.6**	17.6
ClusComp	s4n65500	4.13	9.7	**13.6**	17.7
GPTQ	w3g128	3.13	13.0	19.5	28.4
AWQ	w3g128	3.13	11.7	17.9	**20.2**
ClusComp$^-$	s6n65500	2.87	14.3	16.2	31.9
ClusComp	s6n65500	**2.87**	**10.7**	**15.3**	22.0
GPTQ	w2g128	2.13	83.7	3.1e3	2.0e2
AWQ	w2g128	2.13	1.6e6	2.0e6	2.2e6
ClusComp$^-$	s8n35000	2.14	7.7e2	6.1e3	9.2e2
ClusComp	s8n35000	2.14	**14.6**	**21.8**	**27.5**

Table A.13: The perplexity of the Llama-3-8B backbone in LLaVA-Next-8B, with baseline results from Huang et al. (2024c).

Hyper-parameter	Block-wise error minimization	Recovery training
Optimizer	AdamW (Loshchilov and Hutter, 2019; Kingma and Ba, 2015)	
Weight decay	{0, 0.1, 0.01}	0
LR	{1e-5, 5e-5, 1e-4, 5e-4}	1e-5
LR scheduler	constant	cosine
Warmup ratio	0	0
Max grad norm	-	0.3
Sequence length	2048	4096
Number of samples	128	8192
Epochs	20	1
Batch size	8	8

Table B.1: Hyper-parameters used for the block-wise error minimization and recovery training steps. The underlined settings generally perform well for different scales of LLMs.

Hyper-parameter	WikiText-2	GSM8K	Alpaca-GPT3.5	Alpaca-GPT4
Optimizer	AdamW		AdamW	
Weight decay	0.1		0	
LR	$\{0.7, 1, 3\}\times10^{-4}$		$\{2, 4, 6, 8\}\times10^{-5}$	
LR scheduler	cosine		cosine	
Warmup ratio	3%		6%	
Epochs or max steps	3 epochs	6 epochs	10K steps	2 epochs
Batch size	64	16	16	
Max sequence length	1024	512	2048	

Table B.2: Hyperparameters for the finetuning on Llama-2-7B. The underlined settings generally performs well for different bit levels. We report the average performance from three random runs in this paper.

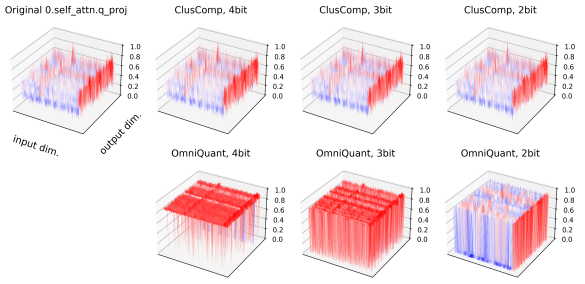

(a) Query projection layer.

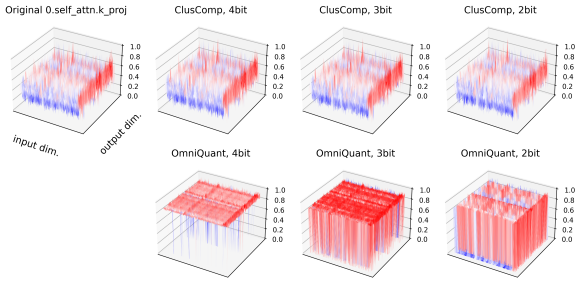

(b) Key projection layer.

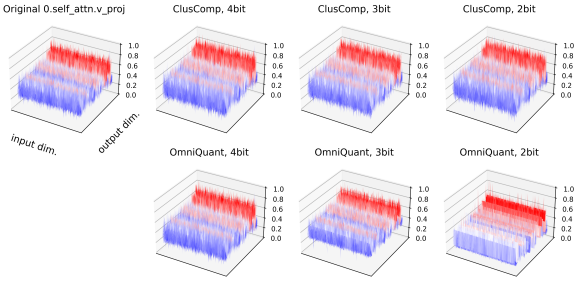

(c) Value projection layer.

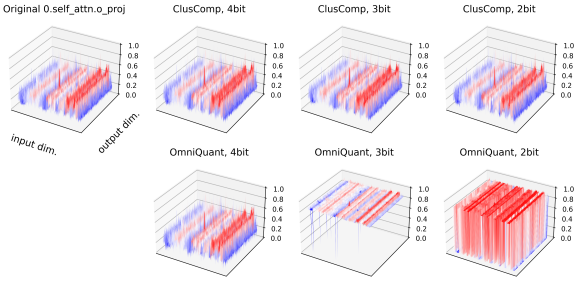

(d) Output projection layer.

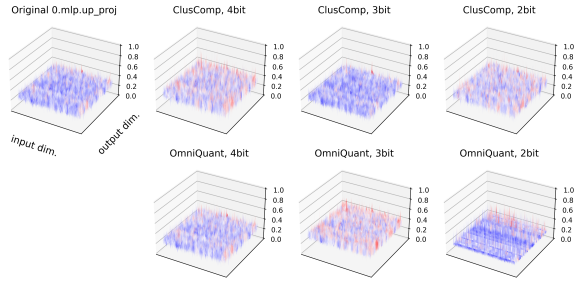

(e) Up projection layer.

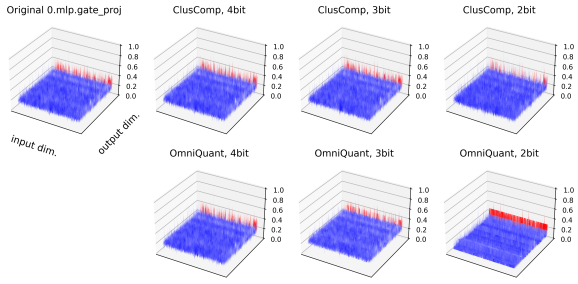

(f) Gate projection layer.

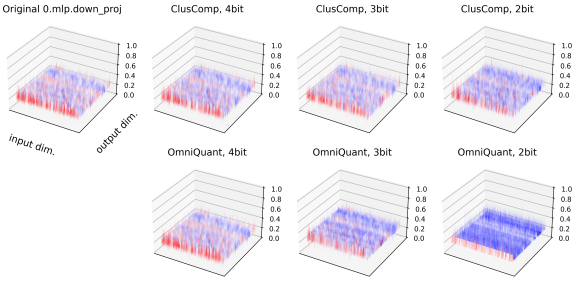

(g) Down projection layer.

Figure A.3: Weight patterns of all layers in the first block (0-th block) of Llama-2-7B. Darker red and blue indicate larger and smaller weight values, respectively. ClusComp's weight distribution of different bit levels can better simulate the original weight distribution.

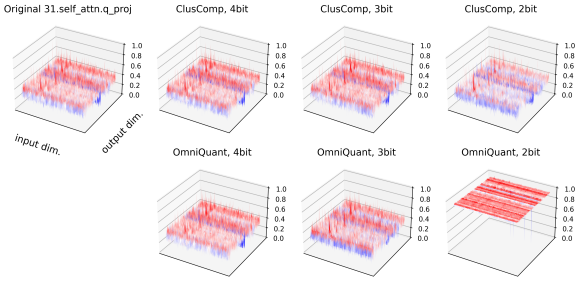

(a) Query projection layer.

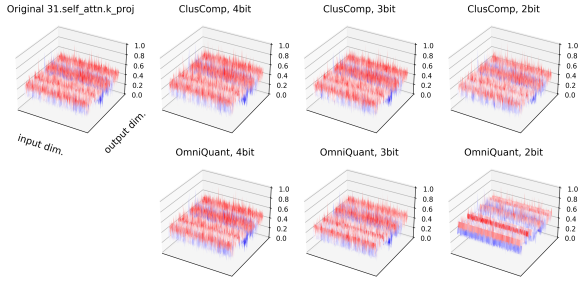

(b) Key projection layer.

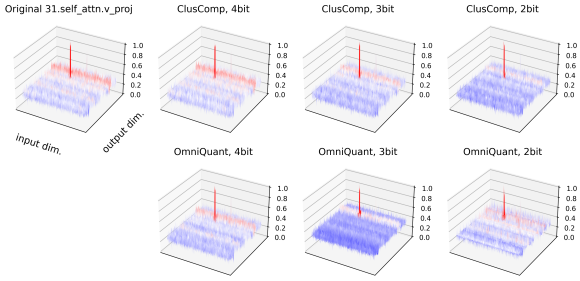

(c) Value projection layer.

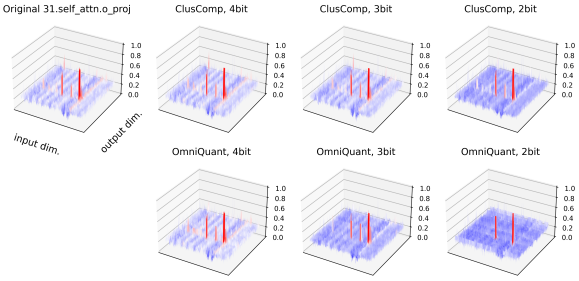

(d) Output projection layer.

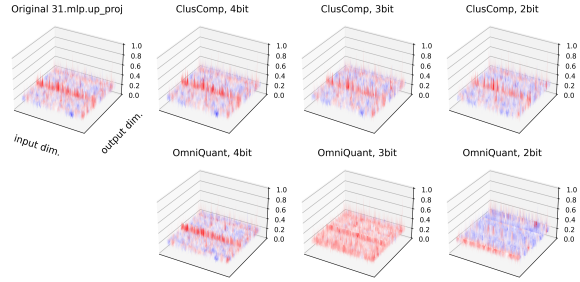

(e) Up projection layer.

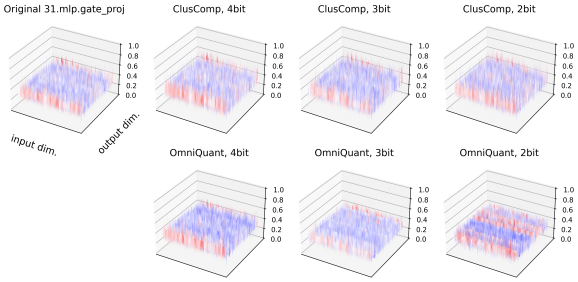

(f) Gate projection layer.

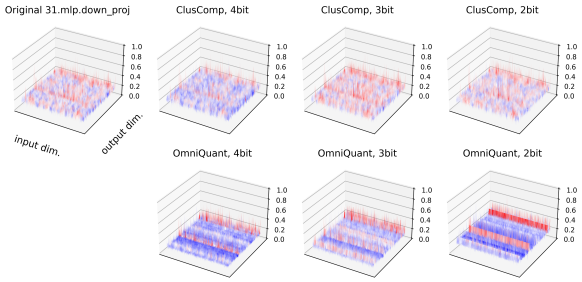

(g) Down projection layer.

Figure A.4: Weight patterns of all layers in the last block (31-st block) of Llama-2-7B. Darker red and blue indicate larger and smaller weight values, respectively. ClusComp's weight distribution of different bit levels can better simulate the original weight distribution.

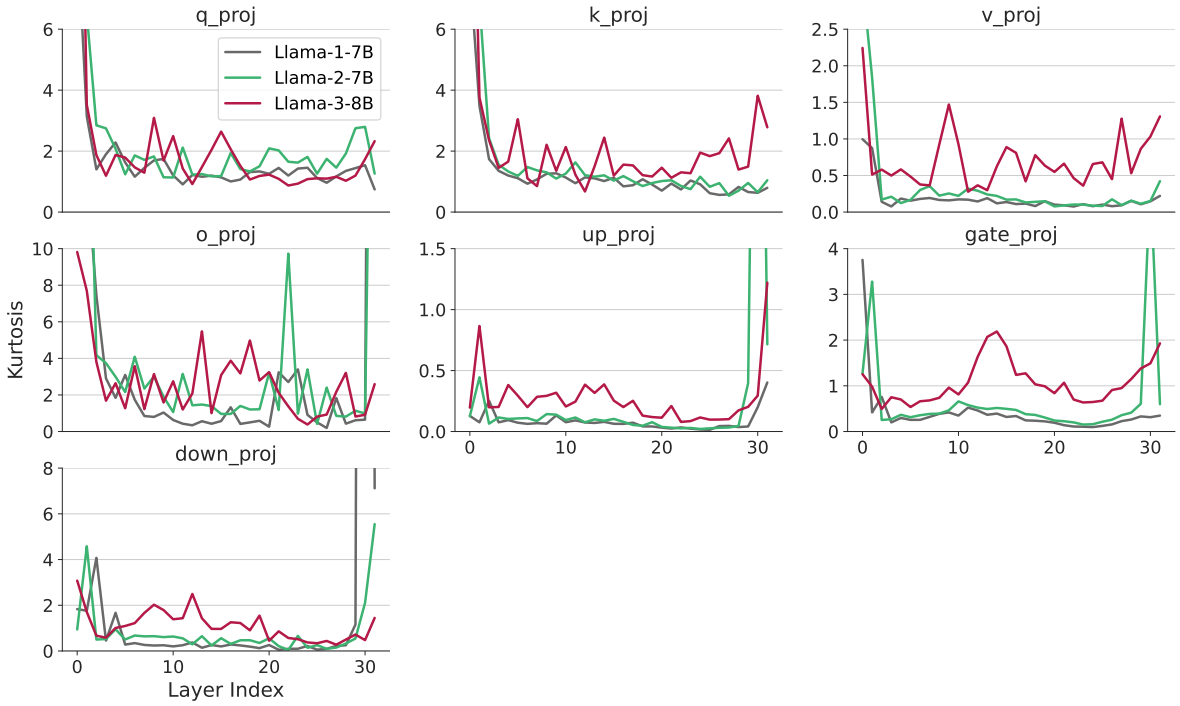

Figure B.1: The kurtosis across various layers in different Llama series reveals three key observations: (1) Layers at either the beginning or the end of LLMs tend to exhibit higher kurtosis values; (2) In the majority of layers, the kurtosis follows a consistent trend across Llama series, with Llama-3 showing the highest values, followed by Llama-2, and then Llama-1; (3) Different types of layers display varying scales of kurtosis, suggesting that a bit allocation strategy that accounts for quantization difficulty could yield better results. We leave the exploration of this idea to future work.

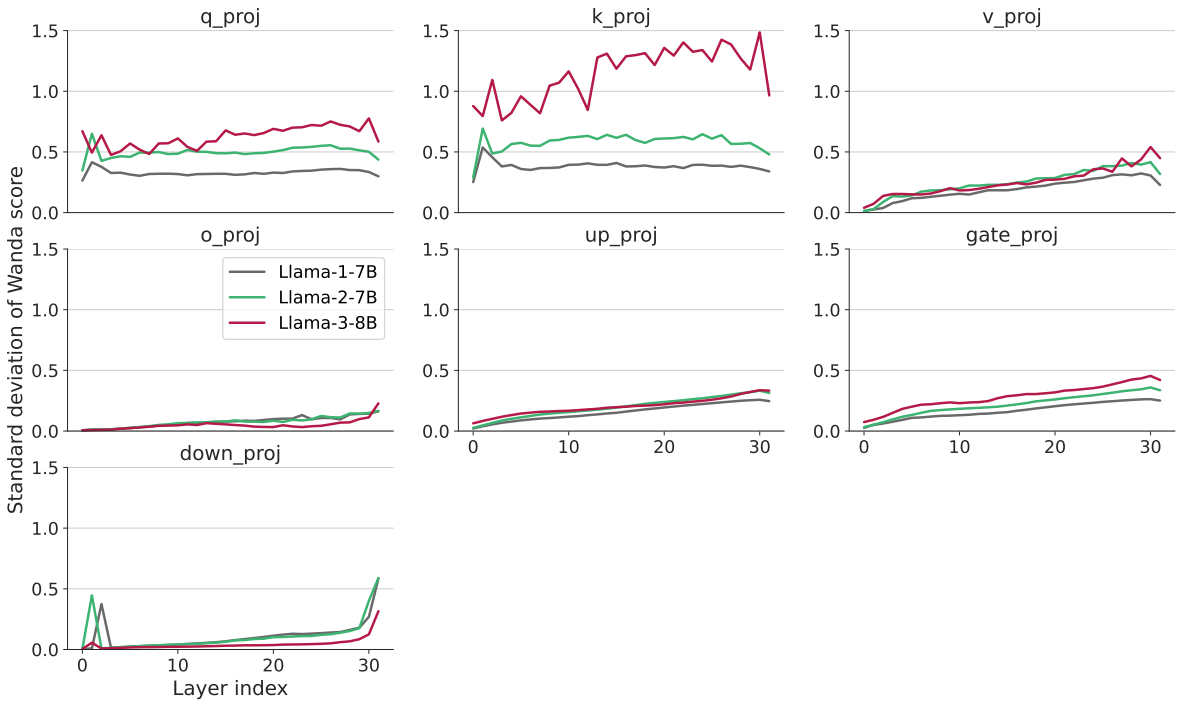

Figure B.2: The standard deviation of Wanda score across various layers in different Llama series reveals three key observations: (1) Deeper layers tend to exhibit higher standard deviation; (2) Three layers (query, key and gate) show a clear trend across Llama series, with Llama-3 showing the highest standard deviation, followed by Llama-2, and then Llama-1; (3) The other four layers show a similar standard deviation for all Llama series.

```python
class ClusCompLinear(nn.Module):
    def __init__(self, in_features, out_features, num_clusters, cluster_dim, bias):
        super().__init__()
        self.out_features = out_features
        self.in_features = in_features
        self.deficiency = out_features % cluster_dim # If the out_features is not dividable by cluster_dim
        if self.deficiency > 0:
            self.deficiency = cluster_dim - self.deficiency

        num_codes = in_features * (out_features + self.deficiency) // cluster_dim
        self.codebook = nn.Parameter(torch.empty((num_clusters, cluster_dim), dtype=torch.bfloat16) # trainable
        code = torch.empty((num_codes,), dtype=torch.uint16)
        self.register_buffer('code', code) # non-trainable
        if bias:
            self.bias = nn.Parameter(torch.empty(out_features))
        else:
            self.register_parameter('bias', None)

    def forward(self, x):
        vectors = self.codebook[self.code]
        if self.deficiency > 0:
            weight = vectors.view(self.in_features, -1)[:, :-self.deficiency]
        else:
            weight = vectors.view(self.in_features, -1)

        if self.bias is not None:
            out = torch.matmul(x, weight) + self.bias
        else:
            out = torch.matmul(x, weight)
        return out
```

Listing 1: PyTorch code for the linear layer of ClusComp. All data type is 16-bit.